microbiology research

MDPI

Article

Revisiting the Phylogeny of Acholeplasmatales and Mollicutes by Codon Usage and Conserved Single-Copy Orthologs Analyses

Anna-Marie Ilic *, Jan Werner Böhm and Michael Kube *

Department of Integrative Infection Biology Crops-Livestock, University of Hohenheim, 70599 Stuttgart, Germany; jan.boehm@uni-hohenheim.de

* Correspondence: annamarie.ilic@uni-hohenheim.de (A.-M.I.); michael.kube@uni-hohenheim.de (M.K.)

Abstract

Increasing genomic data are driving changes in the selection of phylogenetic markers and analysis strategies. Databases enable the extraction of established markers, such as single and multilocus sequence typing (MLST), but are often limited by the number of informative sites or availability with respect to incomplete source data sets or reductive evolution in bacteria such as the *Mollicutes*. Genome-wide analyses like average nucleotide identity (ANI) often overcome these problems but also depend on the alignment percentage. Complementary analyses help validate results and address limitations of primary approaches. However, how genome-wide compositional signals and reduced core gene sets affect phylogenomic resolution across a large and taxonomically diverse dataset of complete *Mollicutes* genomes remains unclear. Therefore, we applied an advanced MLST approach based on single-copy orthologs (SCOs), alongside codon usage analysis. The reliability and impact of these approaches were first analyzed using *Acholeplasmatales* as the foundation, with 16S rRNA gene, ANI, SCOs, and codon usage. Codon usage analysis revealed lineage-associated compositional signatures across the 52 strains that were broadly consistent with current genus and subgroup assignments, whereas ANI and 16S rRNA gene identified species with ≥96.5% and ≥97%, respectively. Among these, SCOs showed the most matches to the current taxonomy, supporting the approach being extended to *Mollicutes*. Applied to 807 *Mollicutes* strains, the analysis revealed 16 shared SCOs. Concatenation of this core set significantly enhanced phylogenomic resolution, providing a robust framework for reconstructing evolutionary relationships within *Mollicutes*.

Keywords: phylogenomics; 16S rRNA gene; ANI; MLST; SCOs

Check for updates

Academic Editor: Tino Polen

Received: 11 February 2026
Revised: 25 March 2026
Accepted: 27 March 2026
Published: 31 March 2026

Copyright: © 2026 by the authors. Licensee MDPI, Basel, Switzerland. This article is an open access article distributed under the terms and conditions of the Creative Commons Attribution (CC BY) license.

1. Introduction

The class *Mollicutes*, the only one within the phylum *Mycoplasmatota*, comprises small wall-less bacteria, characterized by their biological simplicity [1]. The members are associated with diverse hosts, such as animals [2], humans [3,4], plants [5], arthropods [6], and free-living environmental species [7,8], even colonizing extreme environments [9,10]. Genome sequences are available in each group in this bacterial class at different levels of completeness (Table 1). Several species exhibit selective host and tissue preferences. Often, the degree of adaptation is reflected in reductive evolution leading to minimal genomes [11] characterized by low GC content [12] and host-dependent specialized metabolism [13,14]. Considering their Gram-positive origin [15], the diversity of the *Mollicutes* is also reflected in their taxonomic structure [16–18].

Table 1. An overview of the class *Mollicutes*, considering minimum and maximum values for genome size and GC content, along with attributes such as taxonomic classification, number of complete genomes, and typical habitats. Only complete genomes are considered where available; otherwise, literature sources were referenced. The genus *Mycoplasma* is limited to the mycoides group.

Classification	Genome Size (Mbp)	GC Content (mol%)	Level Complete	Habitat
Acholeplasmatales				A, I, P, E
Acholeplasmataceae				
Acholeplasma [1]	1.460–1.611	31.0–32.0	6	
Alteracholeplasma [1]	1.554	29.0	1	
Haploplasma [1]	1.883	28.0	1	
Mariniplasma [1]	1.899	30.0	1	
Paracholeplasma [1]	1.878	36.0	1	
Peloplasma [8]	ND	32.42	0	
'*Candidatus* Phytoplasma' [1,2]	0.499–0.974	20.5–29.0	36	
Anaeroplasmatales				A
Anaeroplasmataceae				
Anaeroplasma [19]	1.500–1.600	29.0–34.0	0	
Asteroleplasma [20]	1.500	~40.0	0	
Haloplasmatales				E
Haloplasmataceae				
Haloplasma [9]	ND	~33.0	0	
Mycoplasmatales				
Sprioplasmataceae				A, I, P, H
Spiroplasma [1]	0.425–2.449	22.5–30.5	126	
'*Candidatus* Mariplasma' [2] [21]	0	0	0	
'*Candidatus* Hepatoplasmataceae' [2]				
'*Candidatus* Hepatoplasma' [1,2]	0.606–0.662	22.5–24.5	4	
'*Candidatus* Tyloplasma' [1,2]	0.615	24.5	1	
Mycoplasmataceae				
'*Candidatus* Moeniiplasma' [2] [22]	0.663–1.228	32.0–34.0	0	
Entomoplasma [1]	0.838	34.5	1	
Haemobartonella [1]	0.920–1.156	35.5–39.0	3	
Mesoplasma [1]	0.739–0.908	26.5–30.0	18	
Mycoplasma [1]	0.833–1.212	23.5–27.0	94	
Williamsoniiplasma [1]	0.868–1.032	28.0–30	3	
Mycoplasmoidales				A, H
Metamycoplasmataceae				
Mesomycoplasma [1]	0.737–2.118	23.0–29.5	107	
Metamycoplasma [1]	0.654–0.906	24.0–30.5	44	
Mycoplasmopsis [1]	0.644–2.508	24.0–29.5	190	
Mycoplasmoidaceae				
'*Candidatus* Hennigella' [1,2] [23]	0.636	31.5	0	
Eperythrozoon [1]	0.564–0.757	27.0–39.5	6	
Malacoplasma [1]	0.619–1.359	24.5–28.5	11	
Mycoplasmoides [1]	0.579–1.222	25.5–40.0	135	
Ureaplasma [1]	0.722–0.874	25.5–26.0	16	

Abbreviations: ND, not determined; A, animals; E, extreme habitat; H, humans; I, insects; P, plants. [1] Data were retrieved from the NCBI genome database (https://www.ncbi.nlm.nih.gov/datasets/genome/, accessed on 7 December 2024). [2] Provisional name used for well-characterized but still uncultured organisms.

The class comprises five orders: *Acholeplasmatales*, *Anaeroplasmatales*, *Haloplasmatales*, *Mycoplasmatales* [18], and the newly proposed order *Mycoplasmoidales* [24]. Each order comprises species with a broad spectrum of different habitats. Some, like the *Acholeplasmatales*, have diverse host-relationships comprising the whole range from free-living environmental bacteria [7,8], commensals [25,26] and pathogens [14]. In contrast, *Anaeroplasmatales* are found associated with animal anaerobic environments, such as the rumen [19]. The order of *Haloplasmatales* also comprises halophilic and extremophilic species adapted to saline

environments [9]. *Mycoplasmatales* and *Mycoplasmoidales* comprise species known to be *predominantly parasitic* and cause numerous diseases in humans and vertebrates, although some species act as commensals or opportunistic pathogens [13,27,28].

Recently, *Mycoplasmatales* has incorporated the previously separated order *Entomoplasmatales* [29], which includes bacteria found in various arthropods and plants [30]. The trivial names "Ureaplasmas", "Entomoplasmas", "Eperythrozoon", "Mesoplasmas", "Mycoplasmas", "Spiroplasmas", "Acholeplasmas", "Asteroleplasmas", "Anaeroplasmas", and "Phytoplasmas" are used for members of their respective genera. While "Mycoplasma" and "Mollicutes" were once used interchangeably for all species within the class, today "Mycoplasma" specifically refers to species within the genus *Mycoplasma*, thereby distinguishing it from the broader class *Mollicutes*.

Understanding evolutionary relationships within this diverse class requires robust phylogenetic methods. Phylogenetic analysis typically relies on the comparison of homologous features, such as conserved genes involved in fundamental processes such as translation, often using single marker genes [31,32]. The use of single markers reduces phylogenetic accuracy, especially in metagenomic studies with incomplete or erroneous data [33]. Furthermore, their low variability limits differentiation between closely related species and their vulnerability to horizontal gene transfer (HGT) can obscure true evolutionary relationships [34,35].

To address this, concatenating multiple genes from different loci can combine evolutionary signals, increase the number of variant sites, and reduce biases from individual genes [36]. This approach has been shown to improve accuracy in phylogenetic reconstruction, even in the face of biological complexities [37,38].

Phylogenetic analysis using the 16S rRNA gene, a widely accepted genetic marker, plays a key role in bacterial taxonomy and has significantly enhanced our understanding of *Mollicutes* evolution, taxonomy, and ecological distribution [13,16,39]. Strains are assigned to species and higher ranks, with species boundaries defined by 16S rRNA gene sequence identity [40,41], a method also used for classifying phytoplasmas into subgroups [42]. Advancements in molecular tools and sequencing technologies have improved classification by detecting subtle genetic differences, particularly using average nucleotide identity (ANI) [43], which is effective for distinguishing closely related species. Genome data of more than 835 strains are available according to the National Center for Biotechnology Information data (NCBI https://www.ncbi.nlm.nih.gov/datasets/genome/, accessed on 7 December 2024). For prokaryotic species assignment, a threshold of 95% genome-wide ANI (gANI) is suggested [44]. This approach is also relevant when classifying phytoplasmas, where the 16S rRNA gene sequence identity should be supported by ANI or at least two housekeeping genes with a sequence identity of at least 98.65%, and for identities exceeding 98.65%, either ANI <95% or three housekeeping genes should be used to ensure accurate species delineation [42]. Improvements have also prompted revisions in the classification of other taxonomic groups within *Mollicutes*, including the reclassification of the polyphyletic genus *Mycoplasma* [24]. Such refinements were based on comprehensive analyses of conserved genomic features, including multiple sequence alignments and conserved signature indels (CSIs), which provide reliable molecular markers for delineating evolutionary relationships [24,29].

While these refinements strengthened prokaryotic taxonomy, challenges persisted, especially at higher taxonomic ranks such as the genus level. Updated minimal standards for genome-based prokaryotic taxonomy place overall genomic relatedness indices (OGRIs) metrics and phylogenomic reconstruction at the center of species and genus delineation [45]. However, reliance on individual OGRI metrics, including average amino acid identity (AAI) and percentage of conserved proteins (POCP), has resulted in unclear genus boundaries,

which could not be resolved, leading to suggestions that some of the newly described genera may be non-monophyletic [46]. Nevertheless, the approach was applied to the genus *Acholeplasma*, resulting in the reclassification of several species into new genera, including *Alteracholeplasma*, *Haploplasma*, *Mariniplasma*, and *Paracholeplasma* [10]. Besides AAI [47] and POCP [48], methods such as core AAI (cAAI) [49], ANI, gANI, and alignment fraction (AF) [44] have been introduced to improve classification at higher taxonomic levels. These methods face challenges, particularly at the genus level, due to the lack of standardized delimitation criteria for classifying prokaryotic genomes [48,50,51].

The increasing reliance on genome-wide analyses that depend on alignment-based approaches, such as the basic local alignment search tool (BLAST) [52], which are often computationally intensive and limited by the alignment percentage, underscores the need for more efficient and accurate approaches to classify prokaryotic genomes [53]. To overcome this problem, methods like FastANI [54], which is based on the minHash algorithm [55] and read mapping, have been developed. FastANI aims to identify reciprocal or orthologous mappings with an 70% identity cutoff, making it faster and more efficient while delivering results comparable to traditional ANI methods [54]. However, this approach has its limitations due to the cutoff, which could pose challenges when applied to genomic data from diverse bacterial species [54], such as the *Mollicutes*, where variability in sequence identity may hinder accurate species classification. To address these limitations, alignment-free methods, such as tetranucleotide frequency analysis [56], offer an alternative strategy by capturing genome-wide signatures that are highly conserved across species [57]. These methods, which do not require complete genome alignment, have been demonstrated to correlate well with ANI and are increasingly being applied for species delineation, offering a promising solution for large-scale genomic analyses [57,58]. However, the ability to distinguish genomic composition increases with the size of the oligonucleotide [59,60], with tetranucleotides being a common choice due to their balance between distinguishing power and computational efficiency [61,62]. One widely used method, the tetranucleotide-derived z-value Pearson correlation coefficient (TETRA), shows that values greater than 0.99, when aligned with ANI values above 95–96%, can support species assignment [62]. However, the reliance on these thresholds and the interdependence between TETRA and ANI values can pose challenges, particularly in cases where the genome composition exhibits higher complexity or greater variability, potentially reducing the accuracy of species delineation [62]. In this context, other oligonucleotide frequency methods, such as pentanucleotide [63] and trinucleotide [64] analyses, have shown superior performance, offering more precise sequence composition with stronger correlations to species' phylogenies and evolutionary relationships.

Given the unique genomic characteristics of the *Mollicutes*, including high AT content and alternative genetic codes, analyzing trinucleotide frequencies could be an effective approach to better understand and classify these species. Within the *Mollicutes*, organisms of the orders *Mycoplasmatales* [65,66] and *Mycoplasmoidales* [67] use genetic code 4, in which the codon UGA encodes tryptophan (Trp) instead of acting as a stop codon. In contrast, *Acholeplasmatales* employ the standard genetic code 11, where UGA is recognized as a stop codon [68]. Together with the pronounced AT richness of their genomes, this variability shapes codon usage patterns, favoring codons enriched in adenine (A) and thymine (T). These biases influence translational efficiency by regulating translation elongation speed, co-translational protein folding [69,70], and mRNA stability through increased mutational susceptibility [71], thereby affecting gene expression and cellular function. Consequently, codon usage patterns not only reflect underlying molecular constraints but also capture evolutionary pressures such as mutational bias and environmental adaptation [72], thereby offering valuable genome-wide insights into how these forces

shape organisms. Comparative analysis of these patterns can reveal evolutionary distances between organisms, as closely related species tend to share similar codon usage profiles [73]. Notably, oligonucleotide frequencies, particularly trinucleotide patterns, exhibit the smallest topological distance to homologous gene-based phylogenies, highlighting their value for phylogenomic reconstruction [64].

Taken together, these observations indicate that genome-wide signals, including codon usage, capture evolutionary constraints complementary to traditional phylogenetic approaches, making them particularly relevant for *Mollicutes* given their extreme AT bias, alternative genetic codes, and persistent taxonomic ambiguities. However, how genome reduction and extensive taxonomic diversity in *Mollicutes* influence core genome definition and phylogenomic resolution remains insufficiently resolved.

We therefore evaluated genome-wide signals derived from codon usage and core single-copy orthologues (SCOs) to re-evaluate the current *Mollicutes* taxonomy, first focusing on complete chromosomes of the *Acholeplasmatales* and subsequently extending the analysis to the class *Mollicutes*. By integrating compositional signals with phylogenomic inference across 807 complete genomes, we examine how reductive evolution constrains SCO retention and impacts phylogenomic resolution.

2. Materials and Methods

2.1. Data Collection

All complete genomes of the class *Mollicutes* were retrieved from the NCBI Genome Database (https://www.ncbi.nlm.nih.gov/datasets/genome/, accessed on 7 December 2024), identifying a total of 835 genomes. Among these 28 genomes were removed ('*Candidatus* Spiroplasma holothuricola' MT37, *Malacoplasma iowae* M821, *Mesomycoplasma hyopneuominae* 13.3A, *M. ovipneumoniae* CHIAS_Crony, *M. ovipneumoniae* OARAU_ATCC1, *M. conjunctivae* NCTC10147, *M. fermentans* NCTC10117, *M. gallinaceum* B2096 8B, *M. genitalium* M6282, *M. hyopneumoniae* NCTC10127, *M. hyorhinis* HUB-1, *M. mycoides* subsp. capri GM12, *M. pneumoniae* M29, *M. pneumoniae* M129, *M. pneumoniae* S55-tet-R, *M. pneumoniae* S68-tet-R, *Mycoplasmoides gallisepticum* k5089, *Mycoplasmopsis bovis* Mb227, *M. synoviae* 5-9, *M. bacterium* LVI A0006, *Mollicutes bacterium* LVI A0039, *M. bacterium* LVI A0075, *M. bacterium* LVI A0078, *Mycoplasma* sp. (ex *Biomphalaria glabrata*) Barreiro1, *Mycoplasmataceae bacterium* AD073, *M. bacterium* AD185, *M. bacterium* AM1032, *M. bacterium* MRE). These exclusions were justified, as the affected genomes showed higher contamination, lower CheckM completeness, and substantially fewer Benchmarking Universal Single-Copy Orthologs (BUSCO) compared to other strains of the same species. By retaining only genomes with low contamination levels, consistently high BUSCO scores, and high CheckM completeness values, we ensured a robust, high-quality, and representative dataset for subsequent analysis. In line with the updated minimal standards for the use of genome data in prokaryotic taxonomy, we selected assemblies that exhibit more than 90% completeness and less than 5% contamination [45]. Extrachromosomal sequences were excluded by manual curation of the genome assemblies.

Two datasets were defined for downstream analyses. The first comprised a subset of 52 *Acholeplasmatales* genomes selected from the 807 complete *Mollicutes* genomes and was used for detailed codon usage and subgroup-level analyses. This subset represented the full set of complete *Acholeplasmatales* genomes available. The second dataset consisted of all 807 genomes and served as a comprehensive phylogenomic framework for the order *Mollicutes*.

2.2. Codon and Amino Acid Usage Analysis

Codon and amino acid usage statistics were carried out using CMG-BioTools v2.2 [74], based on coding sequences (CDS) to examine the frequency and distribution of codons and amino acids across the genomes. To avoid bias, start and stop codons were excluded from the analysis using SeqKit v2.7.0 [75]. The results were visualized in R v4.4.2 [76], employing the package 'd3heatmap' v0.9.0 [77], which generated the heatmap and the dendrograms, and 'viridis' v0.6.5 [78] color palette for enhanced color representation.

2.3. ORF Prediction and Ribosomal Group Assignment

Only chromosomal sequences were retained for analysis, while plasmid sequences were removed. The remaining sequences were then subjected to open reading frame (ORF) prediction and annotation in a uniform manner. The appropriate genetic codes were applied following the current taxonomy [18]: genetic code 11 for *Acholeplasmatales* strains and genetic code 4 for *Mycoplasmatales* and *Mycoplasmoidales* strains. The ORF prediction and annotation were performed using Prodigal v2.6.3 [79]. Additionally, the 16S rRNA genes for *Acholeplasmatales* were identified using RNammer v1.2 [80], for comparative purposes, as this gene serves as a reliable phylogenetic marker, particularly for '*Candidatus* Phytoplasma' species within the order [42]. The assignment of ribosomal groups and subgroups of phytoplasmas was performed by iPhyClassifier [81,82] (https://plantpathology.ba.ars.usda.gov/cgi-bin/resource/iphyclassifier.cgi, accessed on 11 December 2024). In instances where the iPhyClassifier was unable to assign a ribosomal subgroup, a BLASTN v2.16.0 [83] analysis was conducted with an *e*-value cut-off set to e^{-25} and a percentage identity set to 98.65% to verify the subgroup assignment.

2.4. Orthology Analysis and Core Set Identification

An orthology analysis was conducted on all datasets comprising the inferred protein content of 807 sequences from the class *Mollicutes*. After retrieving SCO data sets for each species using BUSCO v5.8.0 [84] with the mollicutes_odb10 comprising 151 SCOs, a core set was manually identified by retaining only those SCOs that were consistently present as complete SCOs across all 807 genomes. This manual curation step was necessary because pseudogenes containing frameshifts can lead to multiple ortholog assignments, thereby limiting the reliability of automated orthology prediction alone. SCO candidates showing duplication, fragmentation, or inconsistent functional annotation across taxa were excluded from the final core set. The selected single-copy orthologs were subsequently validated and cross-checked for functional consistency using BLASTP v2.16.0 [83] with an *e*-value cut-off set to e^{-25} to ensure their accuracy and uniformity across the datasets. For subsequent phylogenomic analyses, the core set was then used to construct concatenated sequences, in which the individual sequences were linked end-to-end while retaining the order provided by the BUSCO output. The orthology results were further validated by classifying all CDS into clusters of orthologous groups (COGs) using COGclassifier v1.0.5 [85].

2.5. Phylogenetic Analysis and Maximum Likelihood Tree Construction

For the phylogenetic analysis, the concatenated sequences were aligned using the MUSCLE v3.8.1511 [86] algorithm for both amino acid and nucleotide sequences, and a separate nucleotide alignment based on the 16S rRNA gene was also performed. Where multiple 16S rRNA gene copies were present, all copies were retained, as inter-operon heterogeneity can be taxonomically informative and support tree stability when only a single representative was available for a subgroup. Model selection and maximum likelihood (ML) tree construction were carried out using IQ-TREE v2.3.6 [87], with the best-fitting DNA or protein model selected according to the lowest Bayesian Information

Criterion (BIC) value for optimal balance between model fit and complexity. The ML trees were constructed with 1000 bootstrap replications, applying a threshold of 70 for statistical significance, and visualized in MEGA v11.0.13 [88].

In addition, taxonomic classification and reference-based phylogenetic placement were performed using Genome Taxonomy Database (GTDB)-Toolkit (Tk) v2.6.1 [89] applying the classification workflow based on the bac120 marker set to provide a standardized framework for comparison with the SCO-based phylogenetic analysis. The resulting phylogenetic tree was visualized using Interactive Tree of Life (iTOL) v7.5 [90].

2.6. Genomic Relatedness Assessment

FastANI v1.34 [54] was used to assess the genomic relatedness of *Mollicutes* strains by calculating ANI. This was compared to the 16S rRNA gene sequence identity, which was calculated using R v4.4.2 [76], with the analysis focused specifically on the order *Acholeplasmatales* to evaluate the correlation between ANI and 16S rRNA identity. Default parameters were used for all software tools unless specified otherwise.

3. Results

3.1. Genomic Signatures and Phylogenetic Insights in Acholeplasmatales

3.1.1. Analysis of Codon Usage and Amino Acid Patterns in Acholeplasmatales

The order of the *Acholeplasmatales* was used as a framework to assess codon performance and amino acid usage, and the results were subsequently compared with the classical 16S rRNA-based phylogeny (Figure 1). The analysis (Figure 2) demonstrated that codon usage captured lineage-associated compositional patterns across the 52 strains, whereas amino acid usage provided lower discriminatory power. Both approaches separated the phytoplasma and Acholeplasma Cluster clearly.

The first major cluster (Figure 2A), derived from codon usage patterns, encompassed the genera *Alteracholeplasma*, *Acholeplasma*, *Haploplasma*, and *Mariniplasma*, while *Paracholeplasma* branched as a separate lineage within this cluster, consistent with previous studies [10]. *Alteracholeplasma palmae* J233 and *Haploplasma axanthum* NCTC10138 exhibited divergent codon usage patterns and branched apart from the core Acholeplasma cluster. This pattern was also supported by 16S rRNA (Figure 1), SCOs (Figure 3), and ANI analyses (Figure 4). In contrast to these analyses, strains *Acholeplasma oculi* 19L and *Mariniplasma anaerobium* Mahy22 were closely aligned, and *Acholeplasma hippikon* NCTC10172 exhibited consistent codon usage patterns, forming a cohesive and distinct subcluster. *A. hippikon* has previously been reported as an outlier together with *Acholeplasma equifetale* within the genus [10,91]. The second major cluster corresponded to the genus '*Candidatus* Phytoplasma', with strains displaying subgroup-specific codon usage profiles. For most strains, codon usage patterns were broadly consistent with current taxonomic assignments [42,92], indicating that compositional signatures can provide complementary information at the subgroup level. Members of subgroup 16SrI (Onion yellows phytoplasma OY-M, '*Ca.* P. asteris' QS2022, '*Ca.* P. asteris' M8, '*Ca.* P. asteris' RP166, Paulownia witches'-broom phytoplasma Zhengzhou, Aster yellows witches'-broom AYWB, '*Ca.* P. asteris' M33, 'Catharanthus roseus' aster yellows phytoplasma De Villa, Maize bushy stunt phytoplasma M3, Mulberry dwarf phytoplasma MDGZ-01) and subgroup 16SrXII ('*Ca.* P. solani' c1, '*Ca.* P. solani' c4, '*Ca.* P. solani' c5, '*Ca.* P. solani' o3, Strawberry lethal yellows phytoplasma (CPA) NZSb11, '*Ca.* P. australiense' PAa) exhibited similar codon usage patterns, consistent with their current subgroup classifications [93]. However, some deviations were observed. The recently described 16SrXII-P subgroup strain '*Ca.* P. solani' GOE showed codon usage similarity to '*Ca.* P. pruni' PR2021 rather than to other 16SrXII strains, highlighting that compositional similarity does not necessarily correspond to taxonomic relatedness [94]. The 16SrII group remained intact and consistent with its expected classification [95]. Flavescence

dorée phytoplasma CH did not cluster with its subgroup members but instead aligned more closely with strains from the 16SrVII subgroup (‘*Ca*. P. fraxini’ AshY1, ‘*Ca*. P.’ sp. ArAWB-2021), forming a distinct cluster. Previous studies have reported clustering of Flavescence dorée phytoplasma with ‘*Ca*. P. rubi’, suggesting a closer phylogenetic relationship between these species [96]. Codon usage analysis further highlighted compositional ambiguities within subgroups 16SrXI and 16SrXIV, as previously observed [92,97]. Specifically, ‘*Ca*. P. oryzae’ HN2022, currently assigned to subgroup 16SrXI, exhibited codon usage patterns more similar to those of ‘*Ca*. P. cynodontis’ GY2015 from subgroup 16SrXIV than to ‘*Ca*. P. sacchari’ SCWL1, another member of 16SrXI.

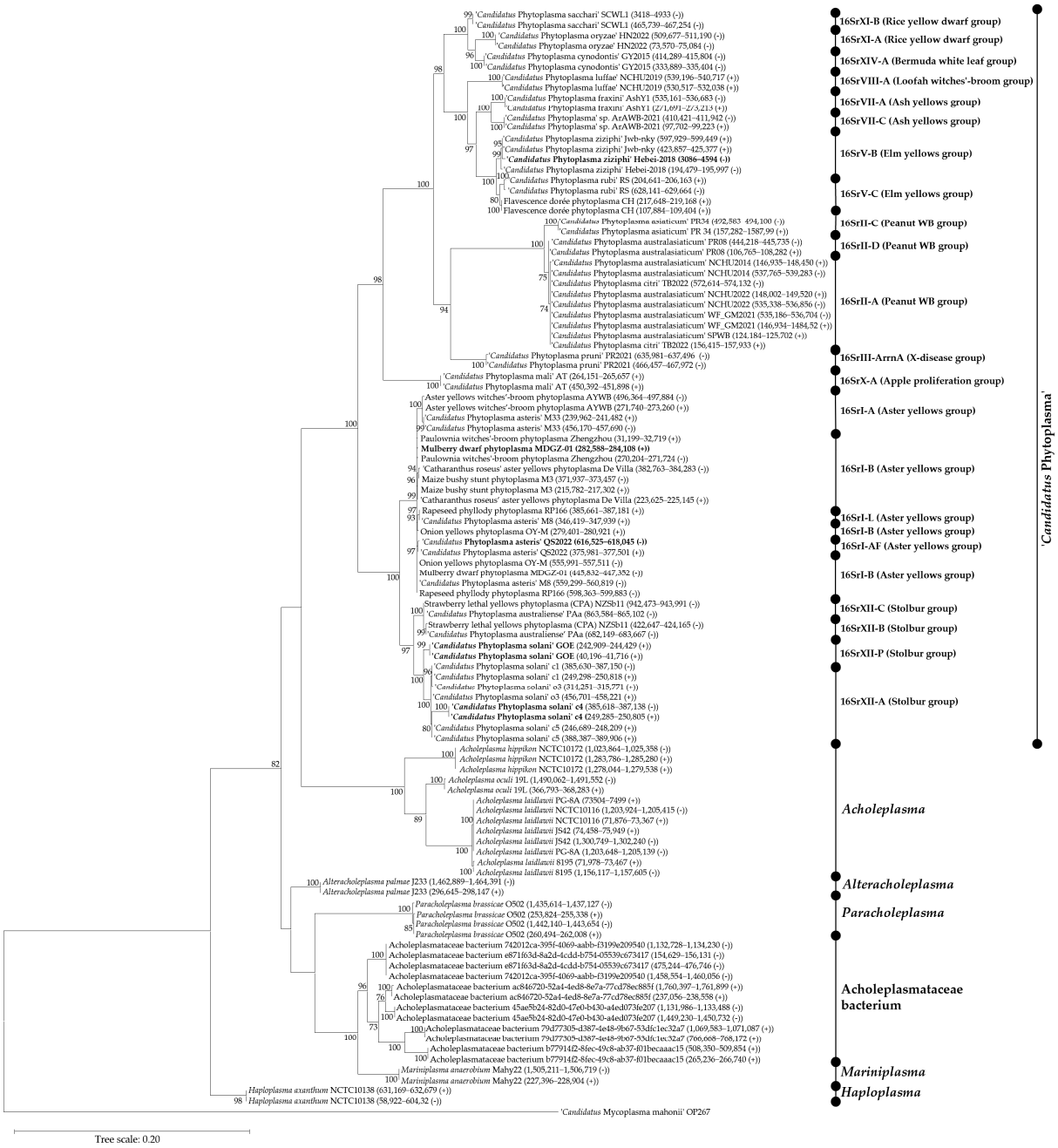


Figure 1. The phylogenetic tree was reconstructed using the full-length 16S rRNA obtained from the genomes of 52 *Acholeplasmatales* strains (gene positions are given in brackets with strand orientation indicated by + and -), aligned using MUSCLE, and inferred by maximum likelihood with IQ-TREE using 1000 bootstrap replicates. ‘*Candidatus* Mycoplasma mahonii’ OP267 was used as the outgroup.

Each phytoplasma strain is assigned to its 16S ribosomal group, with those falling below the 97% cutoff value highlighted in bold. Confidence values greater than 70 (bootstrap percentage) are indicated on the branches. The tree was generated using the GTR + F + I + G4 model, with 1550 positions in the final dataset, of which 509 were variable sites. The tree scale, set at 0.20, represents the number of substitutions per site, indicating evolutionary divergence.

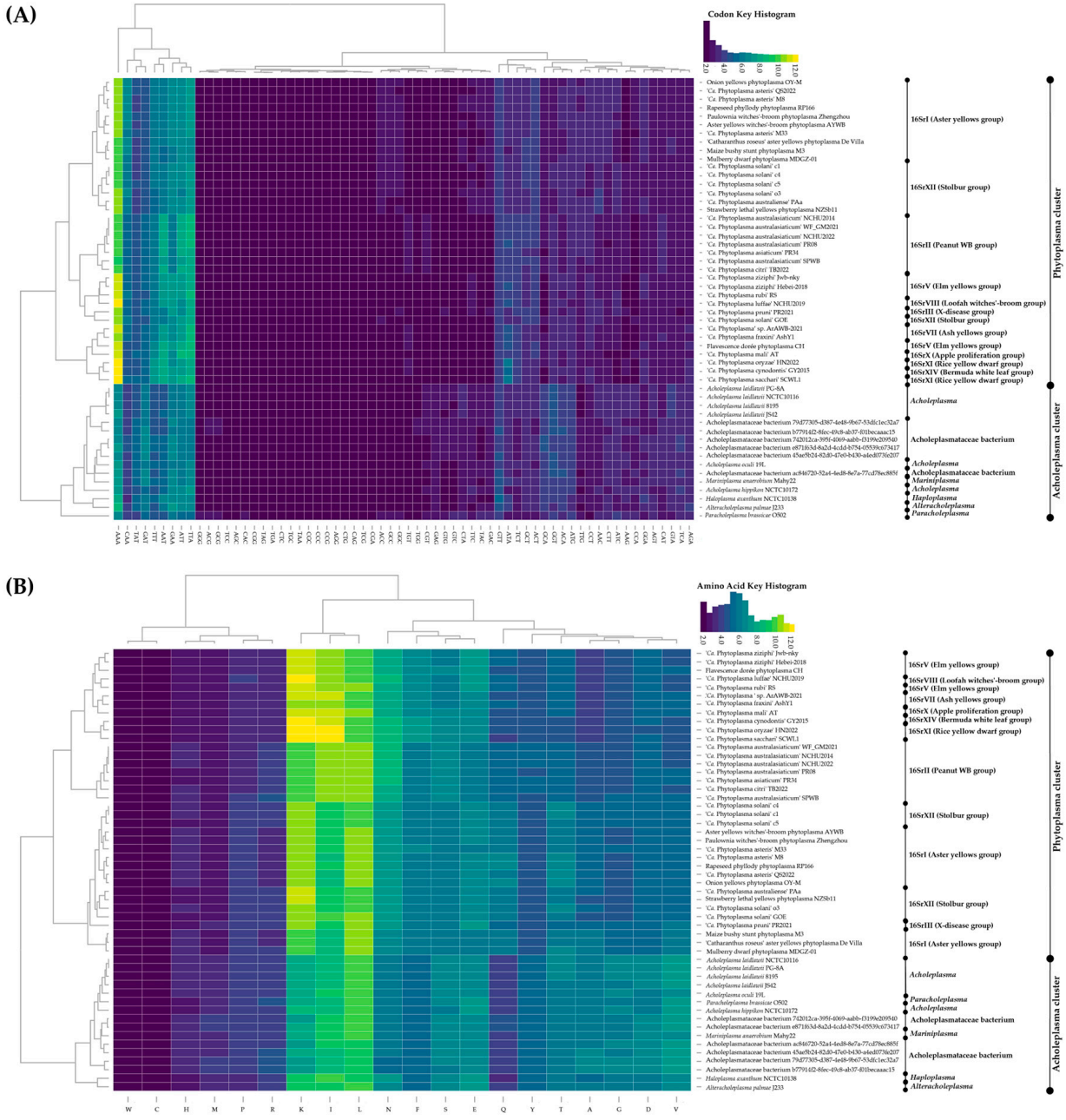


Figure 2. Heatmaps on (**A**) codon usage and (**B**) amino acid usage show codon (amino acid) frequencies of total protein-coding genes of 52 *Acholeplasmatales* strains. Each phytoplasma strain is assigned to its 16S ribosomal group. The heatmaps clustered in two dendrograms, thus reordering the organisms and the codons to show the shortest distance between them. The 64 codons (21 amino acids) are shown along the *x*-axis. The histogram (see key, top right) shows how often each codon occurs. The color intensity changes from dark blue to bright yellow with an increase in the frequency of a particular codon.

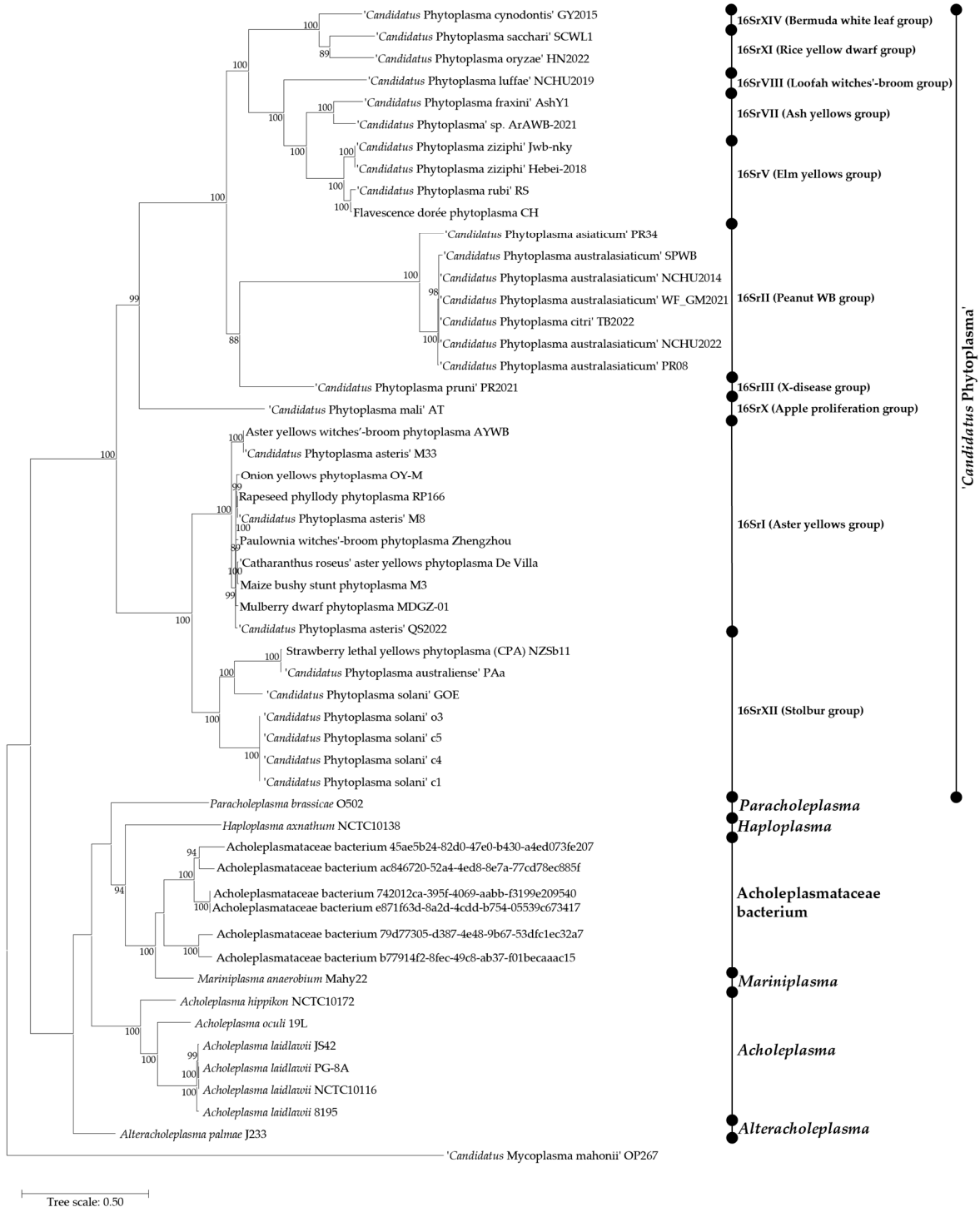


Figure 3. The phylogenomic tree represents the relationships among 52 *Acholeplasmatales* strains and '*Candidatus* Mycoplasma mahonii' OP267 as the root, based on a concatemer from a core set of 16 single-copy orthologs. The sequences were aligned using MUSCLE, and the maximum-likelihood tree was inferred with IQ-TREE using 1000 bootstrap replicates. Each phytoplasma strain is assigned to its 16S ribosomal group. Confidence values greater than 70 (bootstrap percentage) are indicated on the branches. The tree was generated using the LG + F + I + G4 model, with 5386 positions in the final dataset, of which 4430 were variable sites. The tree scale, set at 0.50, represents the number of substitutions per site, indicating evolutionary divergence.

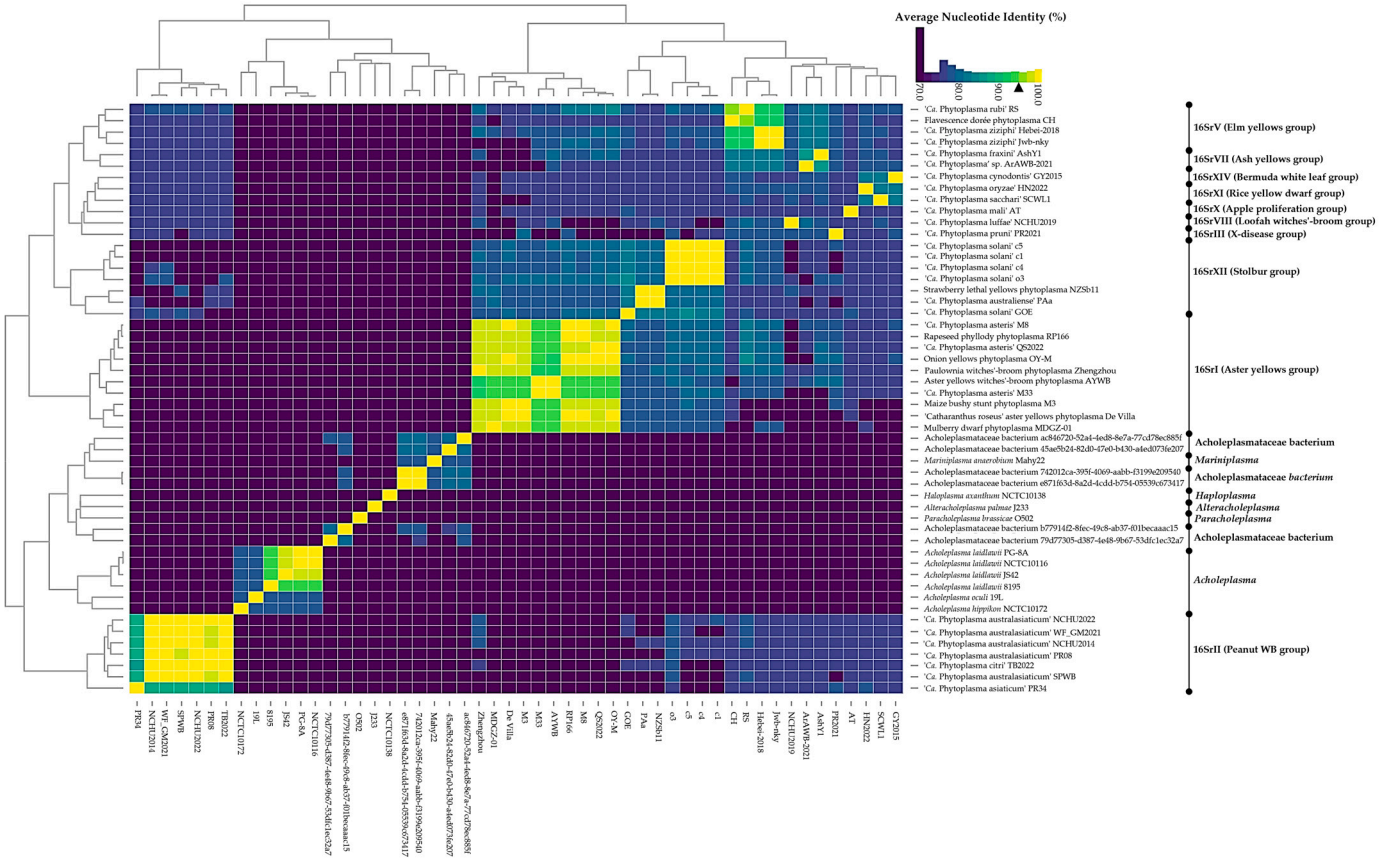


Figure 4. Heatmap illustrating ANI across 52 *Acholeplasmatales* strains. The color intensity represents the degree of nucleotide similarity between the strains, with darker shades indicating lower ANI values. The percentage values are depicted by a heat map (see key, top right). The black arrowhead at the gradient key indicates 95% ANI. On the *x*-axis, the modifier is displayed, while the *y*-axis shows the species with strain names.

To address inconsistencies observed in codon usage-based subgroup assignments, amino acid usage patterns (Figure 2B) were examined as an alternative approach. However, this analysis did not resolve these inconsistencies. Subgroups 16SrI and 16SrXII clustered together rather than forming a distinct separation, reflecting the limited resolution of this approach. The amino acid usage approach was only able to broadly capture the larger clusters, such as the phytoplasma and acholeplasma, without providing sufficient granularity to distinguish subgroups or genera. This reduced resolution was associated with fewer detectable compositional differences at the amino acid level.

3.1.2. Comparing Codon Usage vs. Core SCOs Analysis

To overcome the limited resolution observed in codon- and amino acid usage–based analyses within *Acholeplasmatales* and to place these patterns into a broader phylogenomic context, a complementary approach based on conserved SCOs was applied across the order *Mollicutes* to reassess phylogenetic assignments. In total, 16 SCOs were consistently retained across all 807 complete genomes of the studied *Mollicutes* strains, highlighting their essential roles and high degree of conservation (Table 2). Given the extensive phylogenetic breadth of the dataset and the well-known reductive genome evolution in *Mollicutes*, this small universally shared core was expected and reflects a stringent selection of markers that remained complete, single-copy, and functionally consistent across all taxa. The selected SCOs constitute a curated subset of well-established, conserved universal bacterial single-copy orthologs derived from OrthoDB [98] and do not represent newly identified orthologs.

Functionally, the final set was strongly enriched in essential housekeeping genes, with 13 of the 16 SCOs related to translation and ribosomal functions, and the remaining markers linked to protein quality control, protein targeting, and DNA replication. Thus, the retained SCOs represent a highly conserved phylogenomic framework for comparisons across deeply diverged *Mollicutes* lineages. Ten of these corresponded to ribosomal proteins (Rps), key components of the protein synthesis machinery. Additionally, this group included proteins with specialized functions in translation and RNA metabolism, such as a K-homology domain protein involved in RNA binding and stability [99], cysteine–tRNA ligase responsible for charging tRNAs with amino acids [100], and translation initiation factor IF-2, which aids in the assembly of the ribosomal initiation complex [101]. The remaining three SCOs were involved in protein quality control and DNA metabolism. One encodes an ATP-dependent Lon protease, a key enzyme in protein quality control and stress response through ATP-dependent proteolysis [102]. Another encodes a signal recognition particle protein, crucial for the translocation of secretory and membrane proteins [103]. The last SCO is DNA polymerase III subunit gamma/tau, an essential enzyme for DNA replication and repair [104]. Together, these 16 SCOs underline their essential biological roles and high degree of conservation, enabling robust phylogenetic inference within *Mollicutes*.

Table 2. The specific details of the core single-copy orthologs that were identified in 807 genomes within the *Mollicutes* class are presented here. These include the protein name, BUSCO ID, COG ID, COG category, and annotation.

Protein Name	BUSCO ID	COG ID	COG Category	Annotation
Lon	437at31969	COG0466	O	ATP-dependent Lon protease
Ffh	1285at31969	COG0541	U	Signal recognition particle protein
InfB	1459at31969	COG0532	J	Translation initiation factor IF-2
DnaX	1481at31969	COG2812	L	DNA polymerase III subunit gamma/tau
RplB	2999at31969	COG0090	J	Ribosomal protein L2
CysS	3395at31969	COG0215	J	Cysteine--tRNA ligase
RpsC	4792at31969	COG0092	J	K Homology domain
RplE	5908at31969	COG0094	J	Ribosomal protein L5
RplM	6279at31969	COG0102	J	Ribosomal protein L13
RplP	6835at31969	COG0197	J	Ribosomal protein L16
RpsE	7077at31969	COG0098	J	Ribosomal protein S5
RpsH	7534at31969	COG0096	J	Ribosomal protein S8
RpsK	8165at31969	COG0100	J	Ribosomal protein S11
RplN	8205at31969	COG0093	J	Ribosomal protein L14P
RpsS	8971at31969	COG0185	J	Ribosomal protein S19
RpmE	9756at31969	COG0254	J	Ribosomal protein L31

Abbreviations of COG categories: J = translation, ribosomal structure, and biogenesis; L = replication, recombination, and repair; O = posttranslational modification, protein turnover, chaperones; U = intracellular trafficking, secretion, and vesicular transport.

Phylogenomic analysis based on the core set of 16 SCOs (Figure 3) resolved distinct clusters corresponding to the major genera within *Acholeplasmatales*, including *Acholeplasma*, *Alteracholeplasma*, *Haploplasma*, *Paracholeplasma*, and *Mariniplasma*, as observed in earlier research [10]. SCO-based phylogeny resolved these genera as distinct clusters [105]. At the subgroup level, strains were clustered in accordance with their current taxonomic assignments and showed high bootstrap support across internal nodes, resolving several lineages that appeared ambiguous in marker-based analyses. A small number of strains occupied distinct, well-supported positions, reflecting divergent evolutionary histories within *Acholeplasmatales*.

3.1.3. Comparing the Reliability of the SCO Analysis vs. 16S rRNA and ANI

To evaluate the relative reliability of different phylogenetic approaches, results from codon usage profiling (Figure 2), full-length 16S rRNA analysis (Figure 1), genome-wide ANI analysis (Figure 4), and SCO-based phylogenomics (Figure 3) were compared in a stepwise manner reflecting increasing methodological resolution and phylogenetic specificity. This comparison aimed to assess how effectively each approach resolves relationships within *Acholeplasmatales* across genus, subgroup, and species levels.

The full-length 16S rRNA phylogeny reliably recovered the major taxonomic structure of *Acholeplasmatales* but included only 509 variable sites out of 1550 positions, limiting resolution at finer taxonomic scales. However, its resolving power was limited at finer taxonomic scales, particularly within closely related phytoplasma subgroups. As already highlighted by codon usage analysis (Section 3.1.1), strains assigned to the 16SrXI and 16SrXIV subgroups were not consistently separated, reflecting the high sequence conservation of the 16S rRNA gene. This limitation is further illustrated by the low number of variable sites in the 16S rRNA alignment (509 of 1550 positions). Codon usage analysis improved resolution compared to 16S rRNA alone by capturing lineage-specific genomic signatures (Section 3.1.1). However, because these patterns alone primarily reflect genome-wide mutational and compositional biases rather than shared evolutionary ancestry, their utility for resolving complex subgroup boundaries remained limited.

To further evaluate subgroup-level assignments within the established 16S rRNA–based classification framework, iPhyClassifier analysis was applied as an additional validation tool, providing similarity coefficients for direct comparison with defined 16Sr groups and subgroups, where values ≥97.5% indicate confident subgroup assignment. The iPhyClassifier analysis revealed that the virtual RFLP pattern derived from both copies of the 16S rRNA sequence of '*Ca*. P. solani' GOE differed from the reference patterns of all previously established 16Sr groups and subgroups [106,107]. It showed the highest similarity to the 16Sr XII subgroup I, with a similarity coefficient of 96.0%. Moreover, ANI analysis (Table S2) further supported this observation, as '*Ca*. P. solani' GOE did not cluster within the 16SrXII-A subgroup, exhibiting a maximum ANI value of 83.3% when compared to c5 and a maximum of 82.23% with NZSb11 from the 16SrXII-B/C subgroup, thereby excluding it from the A-type, B/C-type and assigning it to P-type, which is consistent with recent reports [94]. SCO-based phylogenomics resolved GOE as a distinct lineage with full bootstrap support, demonstrating its ability to disentangle complex evolutionary relationships that remain ambiguous under single-marker, composition-based, or similarity-based approaches. Together, these findings are consistent with its proposed recognition as a distinct species [107].

In contrast to the divergent placement of '*Ca*. P. solani' GOE, we next assessed whether genome-wide similarity measures support the conventional subgroup assignments within the remaining 16SrXII strains. ANI values exceeding 95%, a threshold commonly applied in phytoplasma taxonomy, provided strong support for these classifications. For instance, '*Ca*. P. solani' c4 exhibited ANI values above 95% when compared with its closest subgroup members ('*Ca*. P. solani' c1, c5, and o3), supporting its placement within subgroup 16SrXII-A. However, iPhyClassifier analysis assigned c4 a similarity coefficient of 97.0%, which falls marginally below the commonly applied ≥97.5% threshold for confident subgroup assignment. Despite this borderline value, BLASTN analysis of the 16S rRNA gene revealed a sequence identity of 98.75%, and SCO-based phylogenomics placed c4 unambiguously within subgroup 16SrXII-A with full bootstrap support. Coming back to the 16SrXI and 16SrXIV subgroups, ANI analysis (Figure 4) also proved inconclusive at the species level, as '*Ca*. P. sacchari' SCWL1 shared 82.19% ANI with '*Ca*. P. oryzae' HN2022 and 81.76% with '*Ca*. P. cynodontis' GY2015, values that did not clearly resolve the relationship between these

taxa. In contrast, only the SCO-based phylogenomic approach unambiguously resolved these strains, assigning '*Ca*. P. sacchari' SCWL1 and '*Ca*. P. oryzae' HN2022 to subgroup 16SrXI with strong bootstrap support (89%), while clearly separating them from '*Ca*. P. cynodontis' GY2015. Similarly, Mulberry dwarf phytoplasma MDGZ-01, '*Ca*. P. asteris' QS2022, and '*Ca*. P. ziziphi' Hebei-2018 could not be clearly assigned to a specific subgroup based on the 16S rRNA approach, though their classification was supported by ANI values and SCO-based phylogeny. Considering species cutoff values, it was observed that '*Candidatus* Phytoplasma ziziphi' reached an ANI value of 99.85%, '*Candidatus* Phytoplasma solani' (excluding '*Ca*. P. solani' GOE) ranged between 98.40% and 99.99%, '*Candidatus* Phytoplasma australasiaticum' between 96.8% and 99.9%, and '*Candidatus* Phytoplasma australiense' had an ANI value of 98.64%.

Moving from subgroup to genus, strains within '*Candidatus* Phytoplasma' showed ANI values ranging from <70% to 99.99%, making it difficult to establish clear genus boundaries. In contrast, *Alteracholeplasma*, *Haploplasma*, and *Paracholeplasma* shared values consistently below 70%, remaining distinguishable based on ANI. Within the *Acholeplasma* genus, values ranged from 78.1% to 99.99%. Notably, *Acholeplasma hippikon* NCTC10172 exhibited the lowest ANI values when compared to other strains, followed by *Acholeplasma oculi* 19L. This divergence is also reflected in the 16S rRNA (Figure 1) and SCOs phylogenomic trees (Figure 3), where both strains cluster more distantly from other *Acholeplasma* species, with *A. hippikon* showing the greatest separation. The distinct clustering of *A. hippikon* was also highlighted in the codon usage analysis (Figure 2A). In contrast, *Mariniplasma anaerobium* Mahy22 shared the highest ANI (77–78%) with *Acholeplasmataceae* bacteria, a finding that was further corroborated by 16S rRNA analysis (Figure 1), which reinforced the distant positioning of these strains and highlighted the challenge of establishing clear genus boundaries.

In contrast to the core set of 16 SCOs, the phylogenetic tree based on the 16S rRNA gene (Figure 1) failed to completely resolve the separation of the acholeplasmas and phytoplasmas, highlighting the limitations of 16S rRNA analysis. The phylogenomic tree derived from the SCO core set showed higher resolving power than the 16S rRNA tree, based on 4430 variable sites out of 5386 positions, compared with 509 variable sites out of 1550 positions in the 16S rRNA alignment. This enhanced resolution is particularly crucial in cases where the 16S rRNA approach may struggle to clearly define subclade boundaries due to high sequence similarities [108–110].

Based on these results, the core set was subsequently applied for phylogenomic reconstruction across complete *Mollicutes* genomes.

3.2. Enlarged SCO Analysis of Mycoplasmas and Their Closest Relatives

The phylogenomic analysis based on a core set of 16 SCOs across 807 *Mollicutes* strains revealed distinct genetic relationships. The concatenated alignment comprised 9804 positions, including 9095 variable sites (Supplementary Dataset S4). The resulting topology recovered the major divisions previously reported for *Mollicutes* [24,29] and showed high to full bootstrap support across major internal nodes. Furthermore, several species currently classified as *Mycoplasma* clustered with other established genera, indicating placements that differ from their current classification. This overall topology was additionally supported by GTDB-Tk–based phylogenomic reconstruction (Supplementary Figure S1), which provided an independent marker-based and reference-guided framework for comparison and recovered the same major higher-level divisions within *Mollicutes*, although support values were generally lower than in the SCO-based phylogeny. However, automatic GTDB-Tk classifications were not fully consistent in all

cases, likely reflecting limitations of reference-based assignment, including incomplete reference coverage and the use of draft genomes in the GTDB reference framework.

To place these phylogenomic results into the context of whole-genome similarity, the complete ANI analysis across the *Mollicutes* dataset was additionally evaluated (Supplementary Table S2). In contrast to the SCO-based phylogeny, ANI did not allow reliable genus-level delineation across the full dataset. Values among strains assigned to the same genus did not consistently exceed 70% ANI cutoff, and ambiguous or unexpected matches were observed across taxonomic boundaries. For example, '*Candidatus* Phytoplasma sacchari' SCWL1 shared 75.19% with *Spiroplasma litorale* TN-1. Similarly, within *Mesoplasma*, the lowest shared ANI value was 79.39% between *Mesoplasma florum* L1 and *Mesoplasma syrphidae* YJS, whereas *M. florum* L1 showed a similarly high ANI value of 79.06% to *Mycoplasma cottewii* VIS, despite their assignment to different genera. Comparable inconsistencies were also observed among the haemotrophic mycoplasmas. For instance, *Eperythrozoon parvum* Indiana shared 78.99% with *Eperythrozoon suis* KI3806, while no corresponding close matches were observed with *Eperythrozoon ovis*, *Eperythrozoon wenyonii*, or '*Candidatus* Mycoplasma haematolamae'. Thus, ANI proved informative for selected close comparisons, but not for robust genus-level classification across *Mollicutes*.

Within the *Mycoplasmoidales* order, several taxonomic inconsistencies were observed, with some of these having been previously noted in earlier studies [46]. Five species described after 2018 (*Mycoplasma tauri* [111], *Mycoplasma miroungigenitalium* [112], *Mycoplasma seminis* [113], *Mycoplasma nasistruthionis* [114], and *Mycoplasma anserisalpingitidis* [115]) and two species previously described but not yet validly published [24] ("*Mycoplasmopsis corogypsi*", "*Mycoplasmopsis crocodyli*") are currently classified as members of the *Mycoplasma* genus. However, the SCO-based phylogenomic analysis (Figures 5 and 6, Supplementary Dataset S4) places these species within the *Mycoplasmopsis* lineage.

Four newly described species (*Mycoplasma miroungirhinis* [112], *Mycoplasma phocoenae* [112], *Mycoplasma phocoeninasale* [112] and *Mycoplasma struthionis* [114]), along with three species previously described but not yet validly published [24] ("*Metamycoplasma anseris*", "*Metamycoplasma gypis*", "*Metamycoplasma phocae*"), and the validly published *Mycoplasmopsis arginini* [24,116], were found to cluster within the *Metamycoplasma* genus. Alvarez-Ponce et al. [117], previously showed that these species ("*M. anseris*", *M. arginini*, "*M. gypis*", and "*M. phocae*") form part of a phylogenetic cluster that was subsequently designated as *Metamycoplasma* [24]. The placement of *Mycoplasmopsis arginini* within the *Metamycoplasma* lineage has also been previously noted [46]. Likewise, the phylogenetic placement of "*Mycoplasmopsis iguanae*" [24] is consistent with its affiliation to the *Mesomycoplasma* lineage, as previously observed [46,117]. "*Mesomycoplasma mobile*" [24] occupied a unique position alongside *Metamycoplasma sualvi* and *Mesomycoplasma moatsii*, situated between '*Candidatus* Mycoplasma mahonii' and the three novel genera (*Mesomycoplasma*, *Metamycoplasma*, *Mycoplasmopsis*). As shown by Yan et al. [46] for "*Mesomycoplasma mobile*", our study further indicates that *Metamycoplasma sualvi* and *Mesomycoplasma moatsii* also cluster separately, forming a separate lineage distinct from the currently established genera. Furthermore, '*Candidatus* Mycoplasma mahonii' formed a distinct clade [46].

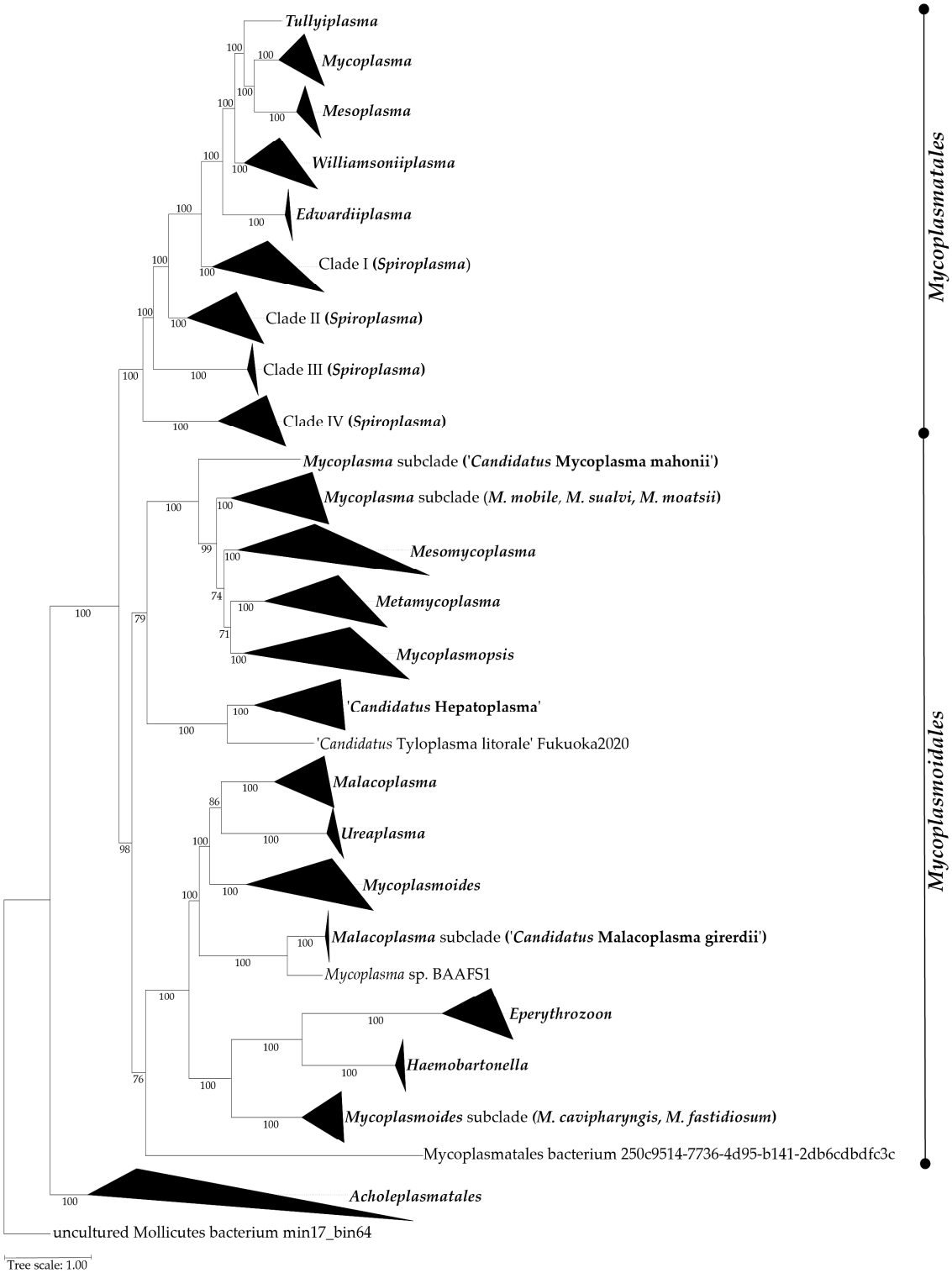


Figure 5. The phylogenetic tree represents the relationships among 807 *Mollicutes* strains and uncultured *Mollicutes bacterium* min17_bin64 as the root, based on a concatemer from a core set of 16 single-copy orthologs. The sequences were aligned using MUSCLE, and the maximum-likelihood tree was inferred with IQ-TREE using 1000 bootstrap replicates. Confidence values greater than 70 (bootstrap percentage) are indicated on the branches. The tree was generated using the VT + F + I + G4 model, with 9804 positions in the final dataset, of which 9095 were variable sites. The tree scale, set at 1.00, represents the number of substitutions per site, indicating evolutionary divergence. Collapsed clusters represent groups of closely related strains corresponding to genera or higher taxonomic levels.

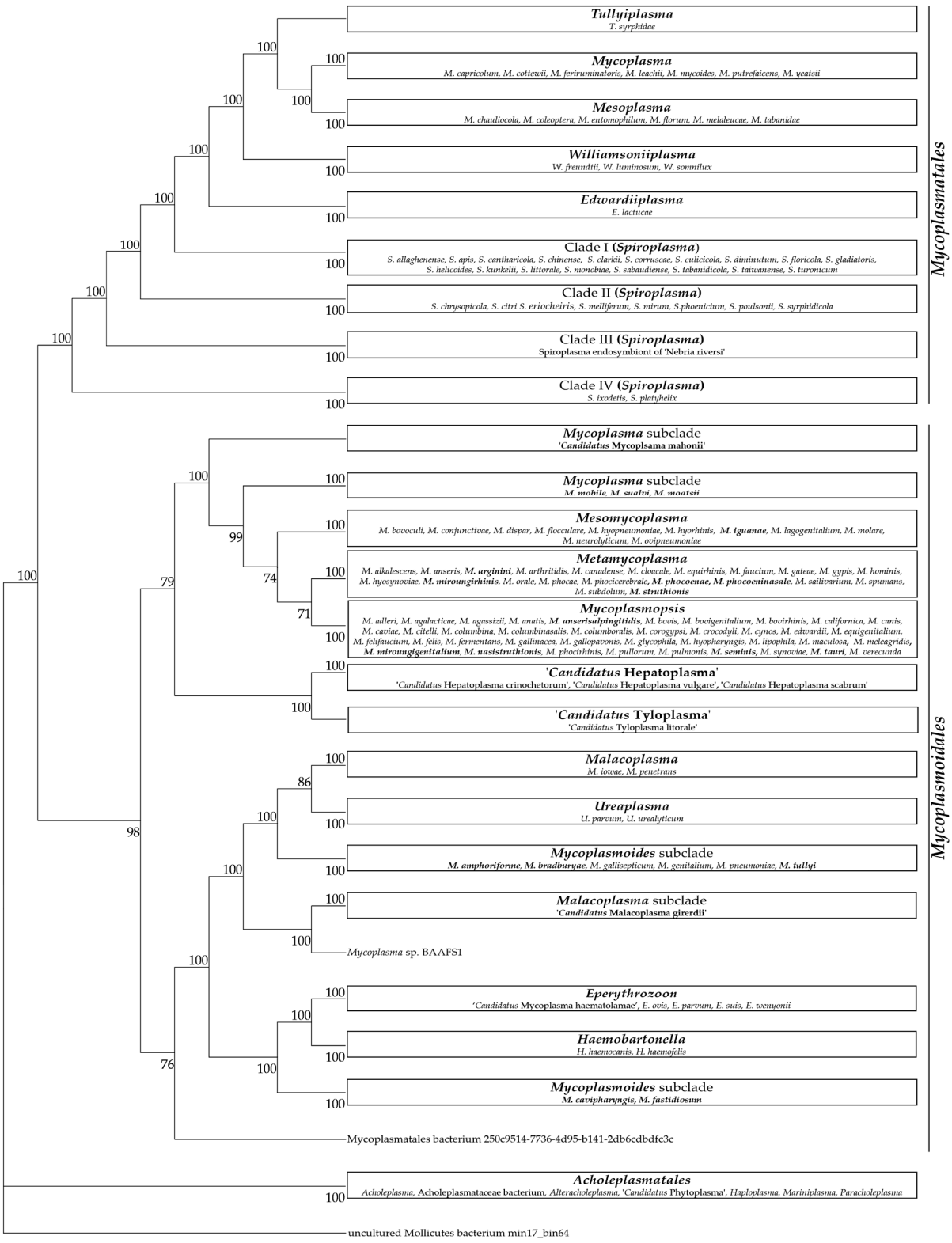


Figure 6. The conceptual consensus tree represents the relationships among 807 *Mollicutes* strains and the uncultured *Mollicutes bacterium* min17_bin64 as the root, based on a concatemer from a core set of 16 single-copy orthologs. The sequences were aligned using MUSCLE, and the maximum-likelihood tree was inferred with IQ-TREE using 1000 bootstrap replicates. Confidence values greater than 70 (bootstrap percentage) are indicated at the branches. The four recognized *Spiroplasma* clades are labeled with clade I to IV, and the four remaining subclades belonging to the order *Mycoplasmoidales* are labeled with names of corresponding genera. The species that have been reclassified in this study are highlighted in bold.

In the case of *Mycoplasmoides*, two newly described species (*Mycoplasma bradburyae* [118] and *Mycoplasma tullyi* [119] were clustered within this genus, while "*Mycoplasmoides amphoriforme*" [24] aligns with the proposed reclassification, though this has yet to be validly published. However, *Mycoplasmoides fastidiosum* [24,116] and "*Mycoplasma cavipharyngis*" [24] were placed within the haemotrophic cluster [120] but could not be assigned to either *Haemobartonella* or *Eperythrozoon*. Additionally, these species were observed to cluster separately from the other *Mycoplasmoides* species [117,120], further highlighting their distinct phylogenetic position within this broader clade, indicating a distinct phylogenetic position within this broader clade.

Moving from *Mycoplasmoidales* to *Mycoplasmatales* order, the phylogeny was consistent with the revised taxonomy [29,46]. The analysis also supports the proposed placement of *Entomoplasma freundtii* within the *Williamsoniiplasma* genus [29,121]. Challenges remain with *Mesoplasma syrphidae* and *Mesoplasma lactucae*, which deviate from the remaining *Mesoplasma* species. As suggested [29], both species appear to belong to separate genera, with *M. syrphidae* aligning with *Tullyiplasma* and *M. lactucae* with *Edwardiiplasma*. Overall, the phylogenetic placement of the genera within the *Mycoplasmatales* aligns with the structure observed in a previous study [122]. The cluster containing *Williamsoniiplasma*, *Mesoplasma*, and *Mycoplasma* corresponds to the Mycoides–Entomoplasmataceae group, distinct from the *Spiroplasma* clades. *Spiroplasma* clade I matches the Apis group, clade II aligns with the Citri–Chrysopicola–Mirum group, clade III represents the unique Nebria riversi group, consisting of endosymbionts, including the spiroplasma endosymbiont of 'Nebria riversi', and clade IV corresponds to the Ixodetis group. In summary, the analysis confirms the clustering patterns from the previous study while also identifying the newly recognized Nebria riversi clade. Nevertheless, the phylogenomic analysis recovered a topology consistent with paraphyly within the order. While the *Spiroplasma* clades II–IV form a cohesive group [122,123], the remaining clade I branch outside the *Spiroplasma* lineage. This pattern was consistent with paraphyly of the order in the inferred topology.

Within the *Acholeplasmatales* order, the phylogenomic analysis (Supplementary Dataset S4) showed that the genera from the Acholeplasma cluster, including *Acholeplasma*, *Alteracholeplasma*, *Haploplasma*, *Mariniplasma* and *Paracholeplasma*, form a cohesive group that clusters separately from the phytoplasmas lineage. These findings are consistent with previous studies showing comparable phylogenetic separation among these genera [10,124] and among subgroups within the genus '*Candidatus* Phytoplasma' [125].

4. Discussion

Accurate classification remains challenging due to gaps in available databases, extensive genetic diversity, and the inherent complexity of many species. Traditional methods based on morphological or metabolic profiling often lack sufficient resolution to distinguish closely related taxa, particularly within species complexes exhibiting overlapping phenotypic characteristics. This challenge is further compounded in the class *Mollicutes*, where no in vitro cultivation is available for a considerable number of lineages, including haemoplasmas and phytoplasmas. As a consequence of limited cultivability and difficulties in capturing diversity among closely related taxa, nucleotide sequence data were integrated early as a central component of polyphasic taxonomy [126].

The challenge of regulating new taxa defined by limited data, such as sequences from uncultivated organisms, led to the introduction of the '*Candidatus*' category as a provisional taxonomic designation. For phytoplasmas, this resulted in the establishment of the provisional genus '*Candidatus* Phytoplasma' [127], in line with the convention for uncultured organisms [126]. Initially grounded in phenotypic traits and serology [128–130], the taxonomy of *Mollicutes* has progressively shifted towards approaches based on 16S

rRNA sequences [39,131]. As emphasized by Stackebrandt [132], advances in molecular techniques, including high-quality 16S rRNA sequencing, rapid DNA typing, and MLST, substantially refined bacterial species concepts. Nevertheless, the resolution of 16S rRNA remains constrained by high conservation and the presence of multiple gene copies, limiting its discriminatory power among closely related taxa [133]. Moving from 16S rRNA-based to genome-based approaches has therefore had profound implications for the classification of *Mollicutes*, revealing previously unrecognized diversity and prompting extensive reclassification in line with evolutionary relationships [134].

A major challenge in classification arises from the genetic plasticity of bacterial genomes. HGT, gene duplications, and mutations generate substantial variability, rendering single-method approaches insufficient to capture the full spectrum of diversity. Comparative genomic analyses have demonstrated extensive chromosomal exchanges between phylogenetically distant mycoplasma species inhabiting the same ecological niches [135,136], challenging earlier assumptions that genome streamlining rather than HGT dominated *Mollicutes* evolution [137,138]. In pathogenic mollicutes, recurrent population bottlenecks during host colonization further enhance the adaptive role of HGT, enabling the adaptation and restoration of deleted or inactivated genes [139]. Given the genetic variability and HGT inherent to *Mollicutes*, a polyphasic approach integrating molecular, phenotypic, and genomic data is crucial for precise and reliable taxonomy. This integrative strategy has driven ongoing revisions of *Mollicutes* nomenclature, leading to proposals [24,29] that have been validly published [116,140] and debated [141]. Recent updates to genome-based taxonomic guidelines further refine these principles by explicitly defining the role of genome-wide analyses in prokaryotic taxonomy. The revised minimal standards emphasize that OGRI thresholds should be interpreted as guidelines rather than absolute criteria and that phylogenomic reconstruction for the resolution of complex or ambiguous taxonomic cases [45]. Complementing these standards, curated genome-based resources such as List of Prokaryotic names with Standing in Nomenclature (LPSN) and Type (Strain) Genome Server (TYGS) underline the importance of standardized genome assemblies and phylogenomic analyses, particularly for taxa represented by draft or incomplete genomes [142].

To reassess *Mollicutes* classification under these standards, we analyzed 807 strains with complete chromosomes. Codon usage was evaluated as a genome-wide, alignment-free signal reflecting mutational bias, selection, and genetic drift [72], which in *Mollicutes* is strongly shaped by genome reduction, lifestyle adaptation, and translational optimization [143]. These patterns are particularly evident within *Acholeplasmatales*, where genomes are predominantly AT-rich and exhibit a pronounced preference for AT-ending codons [144]. Here, codon usage analysis revealed lineage-associated genomic signatures across the 52 phytoplasma strains, with characteristic codon patterns that were broadly consistent with current genus- and subgroup-level assignments. While most '*Candidatus* Phytoplasma' strains clustered consistently with established subgroups, several discrepancies underscore the complexity of subgroup classification. Amino acid usage patterns were far less discriminatory and unsuitable for resolving subgroup or genus-level classifications. Previous studies [143,145] have demonstrated that changes in nucleotide biases, particularly shifts in GC content, strongly correlate with global amino acid composition, molecular weight, and aromaticity of proteins. High-expression genes (HEGs) are shaped by stronger purifying selection, resulting in more conserved amino acid profiles, while low-expression genes (LEGs) show greater variability [146]. Due to functional constraints and redundancy in the genetic code, amino acid composition is inherently less variable and therefore provides limited taxonomic resolution among closely related taxa [147]. By reflecting nucleotide-

level variation, codon usage can provide finer compositional discrimination among closely related taxa than amino acid usage [148].

While we clustered strains into distinct categories based on codon usage, it is important to recognize that this classification is not absolute, but rather a heuristic tool to capture the varying patterns observed across the *Mollicutes* clade. However, these dendrograms lack a meaningful evolutionary distance scale and primarily reflect bi-clustering patterns [149]. To mitigate these limitations, codon usage analysis was integrated with complementary phylogenetic methods, as it cannot substitute for traditional single-marker approaches such as the 16S rRNA gene or OGRIs such as ANI, but rather complements them by providing additional genome-wide compositional information. This integration is particularly important given the saturation effects and functional constraints that limit the discriminatory power of 16S rRNA for closely related taxa [133,150]. Concatenated phylogenomic analyses of conserved genes have therefore become increasingly valuable for improving resolution and reducing bias [37,46].

Building on this rationale, we leveraged uniformly annotated complete chromosomes to conduct a core set analysis across the class *Mollicutes*. To avoid confounding effects from accessory genetic material, the present analysis was restricted to chromosomal sequences, whereas extrachromosomal elements such as plasmids were excluded as non-essential [151]. Previous studies have identified 104 SCOs in 39 *Mollicutes* species [134] and 30 SCOs in 183 *Mollicutes* species [46], demonstrating that the size of the inferred core set decreases as taxon sampling increases. While the increased density of variable sites in SCOs improves differentiation, a limitation becomes apparent when examining more distantly related species. Increased sequence divergence can lead to proteins with similar functions but different evolutionary histories being assigned into different orthogroups, as orthogroup definition prioritizes shared ancestry over functional similarity [152].

Reductive genome evolution, a defining feature of *Mollicutes*, likely underlies the limited size of the recovered core set. This effect is further compounded by the considerable phylogenetic and ecological diversity within the class, which includes lineages with distinct host associations, lifestyles, and evolutionary trajectories. Although the BUSCO lineage dataset for *Mollicutes* comprises 151 conserved single-copy orthologs derived from OrthoDB [98], only 16 SCOs were retained across 807 *Mollicutes* chromosomes for downstream phylogenomic analysis. As BUSCO lineage datasets represent near-universal orthologs expected for a given lineage [84], this reduction is consistent with the extensive gene loss that characterizes *Mollicutes* evolution [46,134,138], in which host-dependent adaptation preferentially preserves essential housekeeping functions while other genes are frequently lost. Accordingly, only a small subset of markers remained consistently single-copy and complete across all taxa, whereas candidates affected by gene loss, duplication, or fragmentation were excluded from the final core set. Consequently, the final SCO set is enriched for highly conserved genes involved in core cellular processes, which provide a robust phylogenetic signal for closely related taxa but may limit resolution for deeper evolutionary relationships or highly divergent lineages.

Validation through integration with 16S rRNA and ANI analyses supports the robustness of this approach for resolving subtle evolutionary relationships among closely related species. The quantitative comparison further supports the higher resolving power of the SCO-based framework, which provided substantially more variable sites than the 16S rRNA alignment (4430/5386 vs. 509/1550 in *Acholeplasmatales*) and 9095 variable sites across the *Mollicutes*-wide dataset. This increased sequence variation provides a broader basis for distinguishing clusters and recovering clades consistent with current genus-level assignments, which is central to the taxonomic resolution addressed in this study. In combination with the high-to-full bootstrap support observed across major inter-

nal nodes, this indicates substantially greater resolving power of the SCO-based framework compared with the 16S rRNA dataset. This strong signal is also consistent with the functional composition of the retained core set. Rps account for most of the inferred core set (10 of 16 SCOs), in line with previous *Mollicutes* core genome analyses demonstrating their low susceptibility to gene loss [134]. As single-copy and essential genes, Rps provide a stable phylogenetic signal and are therefore widely used as markers in both concatenated and single-gene analyses [153]. The comparison with the GTDB-Tk framework indicates that the higher-level *Mollicutes* topology inferred from the retained SCO set is not solely dependent on the specific marker selection used here. At the same time, the lower branch support and occasional inconsistencies in automatic GTDB-Tk assignment suggest that reference-guided classification remains sensitive to database composition and may be less informative for fine-scale taxonomic interpretation than the curated SCO-based framework.

This interpretation is also consistent with current genome-based taxonomic concepts. Although ANI was informative for selected close comparisons, its performance for genus-level delineation across *Mollicutes* was limited. This is consistent with previous work showing that ANI is primarily useful for species-level circumscription and does not provide a universally applicable genus boundary on its own [48,62]. Although an empirical genus demarcation range around 73–74% ANI has been proposed [154], this value should be interpreted together with alignment fraction and phylogenomic context rather than as an absolute cutoff, particularly in taxonomically complex groups such as *Mollicutes*.

Phylogenomic analysis based on this SCO framework corroborated current taxonomy, highlighted species whose present classification may warrant re-evaluation, and revealed previously unrecognized clades with strong bootstrap support (Figure 6). These findings underscore significant challenges in delineating genera within the Hominis-clade, particularly in relation to *Mesomycoplasma*, *Metamycoplasma*, and *Mycoplasmopsis* [46]. Furthermore, many *Mycoplasma* species have not been reassigned to the newly proposed genera and continue to retain the name "Mycoplasma". Even those that have been reclassified are often listed as not validly published. These taxonomic inconsistencies, along with the unresolved question of whether *Mycoplasma* is a polyphyletic group, complicate efforts to reflect evolutionary relationships accurately. This lack of clarity impacts not only evolutionary studies but also research on these species' biological roles, pathogenicity, and treatment strategies. Of particular concern is the fact that seven species described ("*Mycoplasmopsis corogypsi*", "*Mycoplasmopsis crocodyli*", "*Metamycoplasma anseris*", "*Metamycoplasma gypis*", "*Metamycoplasma phocae*", "*Mycoplasmopsis iguanae*", "*Mesomycoplasma mobile*") in 2018 [24] have not yet been incorporated into the revised taxonomy and remain classified as members of *Mycoplasma*. However, their phylogenetic placement in this study is consistent with the positions proposed previously and further suggests that several of the newly described genera may not be monophyletic [46]. Furthermore, the phylogenetic placement of 21 species ('*Candidatus* Mycoplasma mahonii', *Mesomycoplasma moatsii*, "*Mesomycoplasma mobile*", *Metamycoplasma sualvi*, *Mycoplasma anserisalpingitidis*, *Mycoplasma bradburyae*, "*Mycoplasma cavipharyngis*", *Mycoplasma miroungigenitalium*, *Mycoplasma miroungirhinis*, *Mycoplasma nasistruthionis*, *Mycoplasma phocoenae*, *Mycoplasma phocoeninasale*, *Mycoplasma seminis*, *Mycoplasma struthionis*, *Mycoplasma tauri*, *Mycoplasma tullyi*, *Mycoplasmoides fastidiosum*, *Mycoplasmopsis arginini*, "*Mycoplasmopsis corogypsi*", "*Mycoplasmopsis crocodyli*", "*Mycoplasmopsis iguanae*") within the order is not fully consistent with the revised taxonomy and may warrant further taxonomic re-evaluation, including assessment of whether additional genera should be considered to better reflect evolutionary relationships.

Similar challenges are observed in *Mycoplasmatales*, where distinguishing genera such as *Edwardiiplasma*, *Mesoplasma*, *Mycoplasma*, *Tullyiplasma*, and *Williamsoniiplasma* remains difficult due to the close genetic relationships between taxa. The results were congruent

with previous findings [29] and were strongly supported by bootstrap values of 100%, thereby providing additional phylogenomic support for the taxonomic re-evaluation. In consideration of the placement of each group within the phylogenomic tree, the results support further taxonomic re-evaluation of *Mycoplasmatales* in order to address their apparent paraphyly [122,155] and to better reflect evolutionary relationships among its members. One possible interpretation of these results is that *Spiroplasma* clades II–IV may warrant evaluation as distinct genera. This approach would ensure that the genus *Spiroplasma* represents a monophyletic group while acknowledging the genetic and evolutionary divergence among the clades.

The genera within the order *Acholeplasmatales* exhibit clearer delineation compared to other *Mollicutes*, reflecting a comparatively stable taxonomic framework. However, even within the Acholeplasma Cluster, precise taxonomic assignments remain challenging. While ANI, 16S rRNA gene analysis, and codon usage patterns are informative for assessing overall genetic relatedness, they could not resolve all ambiguities at the genus and subgroup levels in the present dataset. This limitation is exemplified by phytoplasma lineages assigned to the 16SrXI and 16SrXIV subgroups, where neither 16S rRNA–based classification nor ANI values alone allowed a reliable distinction between closely related evolutionary lineages. In such cases, the SCO-based phylogenomic analysis offered an additional phylogenomic perspective by integrating signal across multiple conserved loci, which may help to inform taxonomic interpretation where standard metrics yielded inconclusive results. Accordingly, SCO-based phylogenomics serves as a complementary framework that supports established OGRIs in future taxonomic refinement of *Mollicutes*.

5. Conclusions

The challenges encountered in recent taxonomic revisions, where newly proposed genera often lack clear genetic differentiation, underscore the need for more robust classification methods. Current genome-based standards, therefore, emphasize the combined use of OGRI metrics and phylogenomic reconstruction as central references for species delineation, explicitly treating OGRI thresholds as guidelines rather than absolute criteria. Accordingly, the present results demonstrate that a defined core set of 16 SCOs provides a reliable phylogenomic marker for *Mollicutes*, yielding a coherent and reproducible phylogenomic framework. By integrating phylogenomic signal across multiple conserved proteins, this approach aligns with current recommendations for both species- and genus-level classification and reduces bias caused by gene-specific anomalies. Given the high number of publicly available *Mollicutes* draft genomes with weak N_{50} values, the 16 SCO framework represents a valuable option for the analysis of draft sequences. Within this framework, codon usage patterns add a complementary signal that supports taxonomic resolution when integrated with OGRI metrics and phylogenomic reconstruction as part of an integrated genome-based approach.

Supplementary Materials: The following supporting information can be downloaded at https://www.mdpi.com/article/10.3390/microbiolres17040070/s1: Table S1: List of Genome Assemblies used in this study; Table S2: Pairwise ANI values across the analyzed *Mollicutes* genomes. Figure S1: Phylogenetic placement of 807 strains within the *Mollicutes* class using GTDB-Tk. Supplementary Dataset S1: Concatenated SCO alignment used for inferring tree in Figure 3, in fasta format; Supplementary Dataset S2: Maximum likelihood tree based on concatenated SCO used for Figure 3, in newick format; Supplementary Dataset S3: Concatenated SCO alignment used for inferring tree in Figures 5 and 6, in fasta format; Supplementary Dataset S4: Maximum likelihood tree based on concatenated SCO used for Figures 5 and 6, in newick format; Supplementary Dataset S5: Phylogenetic tree inferred from GTDB used for Figure S1, in newick format.

Author Contributions: Conceptualization, M.K.; methodology, A.-M.I., J.W.B. and M.K.; software, A.-M.I. and J.W.B.; validation, A.-M.I., J.W.B. and M.K.; formal analysis, A.-M.I. and J.W.B.; investigation, A.-M.I., J.W.B. and M.K.; data curation, A.-M.I., J.W.B. and M.K.; writing—original draft preparation, A.-M.I., J.W.B. and M.K.; writing—review and editing, A.-M.I., J.W.B. and M.K.; visualization, A.-M.I.; supervision, M.K.; project administration, A.-M.I., J.W.B. and M.K. All authors have read and agreed to the published version of the manuscript.

Funding: This research received no external funding.

Institutional Review Board Statement: Not applicable.

Informed Consent Statement: Not applicable.

Data Availability Statement: The datasets generated and analyzed during the current study are available in the NCBI genome database and can be accessed through the accession numbers, which are listed in the Supplementary Materials.

Conflicts of Interest: The authors declare no conflicts of interest.

References

1. Peterson, S.N.; Fraser, C.M. The Complexity of Simplicity. *Genome Biol.* **2001**, *2*, comment2002.1. [CrossRef]
2. Nocard, E.; Roux, E. Le Microbe de La Péripneumonie. *Ann. Anst. Pasteur* **1898**, 240–262.
3. Eaton, M.D.; Meikeljohn, G.; VanHerick, W.; Talbot, J.C. An Infectious Agent from Cases of Atypical Pneumonia Apparently Transmissible to Cotton Rats. *Science* **1942**, *96*, 518–519. [CrossRef]
4. Marmion, B.P. Eaton Agent—Science and Scientific Acceptance: A Historical Commentary. *Clin. Infect. Dis.* **1990**, *12*, 338–353. [CrossRef]
5. Doi, Y.; Teranaka, M.; Yora, K.; Asuyama, H. Mycoplasma- or PLT Group-like Microorganisms Found in the Phloem Elements of Plants Infected with Mulberry Dwarf, Potato Witches' Broom, Aster Yellows, or Paulownia Witches' Broom. *Jpn. J. Phytopathol.* **1967**, *33*, 259–266. [CrossRef]
6. Nasu, S.; Sugiura, M.; Wakimoto, T.; Iida, T. On the Etiologic Agent of Rice Yellow Dwarf Disease. *Ann. Phytopathol. Soc. Jpn.* **1967**, *33*, 343–344.
7. Laidlaw, P.P.; Elford, W.J. A New Group of Filterable Organisms. *Proc. R. Soc. Lond. B Biol. Sci.* **1936**, *120*, 292–303. [CrossRef]
8. Khomyakova, M.A.; Merkel, A.Y.; Novikov, A.A.; Slobodkin, A.I. *Peloplasma aerotolerans* gen. nov., sp. nov., a Novel Anaerobic Free-Living Mollicute Isolated from a Terrestrial Mud Volcano. *Life* **2024**, *14*, 563. [CrossRef]
9. Antunes, A.; Alam, I.; El Dorry, H.; Siam, R.; Robertson, A.; Bajic, V.B.; Stingl, U. Genome Sequence of *Haloplasma contractile*, an Unusual Contractile Bacterium from a Deep-Sea Anoxic Brine Lake. *J. Bacteriol.* **2011**, *193*, 4551–4552. [CrossRef]
10. Watanabe, M.; Kojima, H.; Okano, K.; Fukui, M. *Mariniplasma anaerobium* gen. nov., sp. nov., a Novel Anaerobic Marine Mollicute, and Proposal of Three Novel Genera to Reclassify Members of *Acholeplasma* Clusters II–IV. *Int. J. Syst. Evol. Microbiol.* **2021**, *71*, 005138. [CrossRef] [PubMed]
11. Fraser, C.M.; Gocayne, J.D.; White, O.; Adams, M.D.; Clayton, R.A.; Fleischmann, R.D.; Bult, C.J.; Kerlavage, A.R.; Sutton, G.; Kelley, J.M.; et al. The Minimal Gene Complement of *Mycoplasma genitalium*. *Science* **1995**, *270*, 397–403. [CrossRef]
12. Bové, J.M. Molecular Features of *Mollicutes*. *Clin. Infect. Dis.* **1993**, *17*, S10–S31. [CrossRef] [PubMed]
13. Razin, S.; Yogev, D.; Naot, Y. Molecular Biology and Pathogenicity of Mycoplasmas. *Microbiol. Mol. Biol. Rev.* **1998**, *62*, 1094–1156. [CrossRef]
14. Kube, M.; Mitrovic, J.; Duduk, B.; Rabus, R.; Seemüller, E. Current View on Phytoplasma Genomes and Encoded Metabolism. *Sci. World J.* **2011**, *2012*, 185942. [CrossRef]
15. Gibbons, N.E.; Murray, R.G.E. Proposals Concerning the Higher Taxa of Bacteria. *Int. J. Syst. Bacteriol.* **1978**, *28*, 1–6. [CrossRef]
16. Johansson, K.-E.; Pettersson, B. Taxonomy of *Mollicutes*. In *Molecular Biology and Pathogenicity of Mycoplasmas*; Razin, S., Herrmann, R., Eds.; Springer: New York, NY, USA, 2002; pp. 1–29.
17. Brown, D.R.; Whitcomb, R.F.; Bradbury, J.M. Revised Minimal Standards for Description of New Species of the Class *Mollicutes* (Division Tenericutes). *Int. J. Syst. Evol. Microbiol.* **2007**, *57*, 2703–2719. [CrossRef]
18. Brown, D.R.; May, M.; Bradbury, J.M.; Johansson, K.-E. *Mollicutes*. In *Bergey's Manual of Systematics of Archaea and Bacteria*; John Wiley & Sons, Ltd.: Hoboken, NJ, USA, 2018; pp. 1–11.
19. Brown, D.R.; Bradbury, J.M.; Johansson, K.-E. Anaeroplasma. In *Bergey's Manual of Systematics of Archaea and Bacteria*; John Wiley & Sons, Ltd.: Hoboken, NJ, USA, 2015; pp. 1–5.
20. Brown, D.R.; Bradbury, J.M.; Johansson, K.-E. Asteroleplasma. In *Bergey's Manual of Systematics of Archaea and Bacteria*; John Wiley & Sons, Ltd.: Hoboken, NJ, USA, 2015; pp. 1–3.

21. Ohdera, A.H.; Mansbridge, M.; Wang, M.; Naydenkov, P.; Kamel, B.; Goentoro, L. The Microbiome of a Pacific Moon Jellyfish *Aurelia coerulea*. *PLoS ONE* **2024**, *19*, e0298002. [CrossRef] [PubMed]
22. Naito, M.; Desirò, A.; González, J.B.; Tao, G.; Morton, J.B.; Bonfante, P.; Pawlowska, T.E. '*Candidatus* Moeniiplasma glomeromycotorum', an Endobacterium of Arbuscular Mycorrhizal Fungi. *Int. J. Syst. Evol. Microbiol.* **2017**, *67*, 1177–1184. [CrossRef]
23. Gilroy, R.; Leng, J.; Ravi, A.; Adriaenssens, E.M.; Oren, A.; Baker, D.; Ragione, R.M.L.; Proudman, C.; Pallen, M.J. Metagenomic Investigation of the Equine Faecal Microbiome Reveals Extensive Taxonomic Diversity. *PeerJ* **2022**, *10*, e13084. [CrossRef]
24. Gupta, R.S.; Sawnani, S.; Adeolu, M.; Alnajar, S.; Oren, A. Phylogenetic Framework for the Phylum Tenericutes Based on Genome Sequence Data: Proposal for the Creation of a New Order *Mycoplasmoidales* ord. nov., Containing Two New Families *Mycoplasmoidaceae* fam. nov. and *Metamycoplasmataceae* fam. nov. Harbouring *Eperythrozoon*, *Ureaplasma* and Five Novel Genera. *Antonie van Leeuwenhoek* **2018**, *111*, 1583–1630. [CrossRef]
25. Tully, J.G.; Whitcomb, R.F.; Rose, D.L.; Bové, J.M.; Carle, P.; Somerson, N.L.; Williamson, D.L.; Eden-Green, S. *Acholeplasma brassicae* sp. nov. and *Acholeplasma palmae* sp. nov., Two Non-Sterol-Requiring *Mollicutes* from Plant Surfaces. *Int. J. Syst. Evol. Microbiol.* **1994**, *44*, 680–684. [CrossRef]
26. Martini, M.; Marcone, C.; Lee, I.-M.; Firrao, G. The Family *Acholeplasmataceae* (Including Phytoplasmas). In *The Prokaryotes: Firmicutes and Tenericutes*; Rosenberg, E., DeLong, E.F., Lory, S., Stackebrandt, E., Thompson, F., Eds.; Springer: Berlin/Heidelberg, Germany, 2014; pp. 469–504.
27. Citti, C.; Blanchard, A. Mycoplasmas and Their Host: Emerging and Re-Emerging Minimal Pathogens. *Trends Microbiol.* **2013**, *21*, 196–203. [CrossRef]
28. Shil, P.K.; Wawegama, N.K.; Browning, G.F.; Noormohammadi, A.H.; Marenda, M.S. Mycoplasmas. In *Pathogenesis of Bacterial Infections in Animals*; John Wiley & Sons, Ltd.: Hoboken, NJ, USA, 2022; pp. 667–700.
29. Gupta, R.S.; Son, J.; Oren, A. A Phylogenomic and Molecular Markers Based Taxonomic Framework for Members of the Order *Entomoplasmatales*: Proposal for an Emended Order *Mycoplasmatales* Containing the Family *Spiroplasmataceae* and Emended Family *Mycoplasmataceae* Comprised of Six Genera. *Antonie van Leeuwenhoek* **2019**, *112*, 561–588. [CrossRef]
30. Gasparich, G.E.; Brown, D.R. *Entomoplasmataceae*. In *Bergey's Manual of Systematics of Archaea and Bacteria*; John Wiley & Sons, Ltd.: Hoboken, NJ, USA, 2021; pp. 1–2.
31. Fitz Gibbon, S.T.; House, C.H. Whole Genome-Based Phylogenetic Analysis of Free-Living Microorganisms. *Nucleic Acids Res.* **1999**, *27*, 4218–4222. [CrossRef]
32. Snel, B.; Bork, P.; Huynen, M.A. Genome Phylogeny Based on Gene Content. *Nat. Genet.* **1999**, *21*, 108–110. [CrossRef] [PubMed]
33. Bowers, R.M.; Kyrpides, N.C.; Stepanauskas, R.; Harmon-Smith, M.; Doud, D.; Reddy, T.B.K.; Schulz, F.; Jarett, J.; Rivers, A.R.; Eloe-Fadrosh, E.A.; et al. Minimum Information about a Single Amplified Genome (MISAG) and a Metagenome-Assembled Genome (MIMAG) of Bacteria and Archaea. *Nat. Biotechnol.* **2017**, *35*, 725–731. [CrossRef] [PubMed]
34. Gogarten, J.P.; Doolittle, W.F.; Lawrence, J.G. Prokaryotic Evolution in Light of Gene Transfer. *Mol. Biol. Evol.* **2002**, *19*, 2226–2238. [CrossRef] [PubMed]
35. Creevey, C.J.; Doerks, T.; Fitzpatrick, D.A.; Raes, J.; Bork, P. Universally Distributed Single-Copy Genes Indicate a Constant Rate of Horizontal Transfer. *PLoS ONE* **2011**, *6*, e22099. [CrossRef]
36. Leigh, J.W.; Susko, E.; Baumgartner, M.; Roger, A.J. Testing Congruence in Phylogenomic Analysis. *Syst. Biol.* **2008**, *57*, 104–115. [CrossRef]
37. Gadagkar, S.R.; Rosenberg, M.S.; Kumar, S. Inferring Species Phylogenies from Multiple Genes: Concatenated Sequence Tree versus Consensus Gene Tree. *J. Exp. Zool. B Mol. Dev. Evol.* **2005**, *304*, 64–74. [CrossRef]
38. Ciccarelli, F.D.; Doerks, T.; von Mering, C.; Creevey, C.J.; Snel, B.; Bork, P. Toward Automatic Reconstruction of a Highly Resolved Tree of Life. *Science* **2006**, *311*, 1283–1287. [CrossRef]
39. Woese, C.R.; Maniloff, J.; Zablen, L.B. Phylogenetic Analysis of the Mycoplasmas. *Proc. Natl. Acad. Sci. USA* **1980**, *77*, 494–498. [CrossRef] [PubMed]
40. Stackebrandt, E.; Goebel, B.M. Taxonomic Note: A Place for DNA-DNA Reassociation and 16S rRNA Sequence Analysis in the Present Species Definition in Bacteriology. *Int. J. Syst. Evol. Microbiol.* **1994**, *44*, 846–849. [CrossRef]
41. Hugenholtz, P.; Chuvochina, M.; Oren, A.; Parks, D.H.; Soo, R.M. Prokaryotic Taxonomy and Nomenclature in the Age of Big Sequence Data. *ISME J.* **2021**, *15*, 1879–1892. [CrossRef]
42. Bertaccini, A.; Arocha-Rosete, Y.; Contaldo, N.; Duduk, B.; Fiore, N.; Montano, H.G.; Kube, M.; Kuo, C.-H.; Martini, M.; Oshima, K.; et al. Revision of the '*Candidatus* Phytoplasma' Species Description Guidelines. *Int. J. Syst. Evol. Microbiol.* **2022**, *72*, 005353. [CrossRef]
43. Kim, M.; Oh, H.-S.; Park, S.-C.; Chun, J. Towards a Taxonomic Coherence between Average Nucleotide Identity and 16S rRNA Gene Sequence Similarity for Species Demarcation of Prokaryotes. *Int. J. Syst. Evol. Microbiol.* **2014**, *64*, 346–351. [CrossRef]
44. Varghese, N.J.; Mukherjee, S.; Ivanova, N.; Konstantinidis, K.T.; Mavrommatis, K.; Kyrpides, N.C.; Pati, A. Microbial Species Delineation Using Whole Genome Sequences. *Nucleic Acids Res.* **2015**, *43*, 6761–6771. [CrossRef]

45. Riesco, R.; Trujillo, M.E. Update on the Proposed Minimal Standards for the Use of Genome Data for the Taxonomy of Prokaryotes. *Int. J. Syst. Evol. Microbiol.* **2024**, *74*, 006300. [CrossRef] [PubMed]
46. Yan, X.-H.; Pei, S.-C.; Yen, H.-C.; Blanchard, A.; Sirand-Pugnet, P.; Baby, V.; Gasparich, G.E.; Kuo, C.-H. Delineating Bacterial Genera Based on Gene Content Analysis: A Case Study of the Mycoplasmatales–Entomoplasmatales Clade within the Class *Mollicutes*. *Microb. Genom.* **2024**, *10*, 001321. [CrossRef] [PubMed]
47. Konstantinidis, K.T.; Tiedje, J.M. Towards a Genome-Based Taxonomy for Prokaryotes. *J. Bacteriol.* **2005**, *187*, 6258–6264. [CrossRef]
48. Qin, Q.-L.; Xie, B.-B.; Zhang, X.-Y.; Chen, X.-L.; Zhou, B.-C.; Zhou, J.; Oren, A.; Zhang, Y.-Z. A Proposed Genus Boundary for the Prokaryotes Based on Genomic Insights. *J. Bacteriol.* **2014**, *196*, 2210–2215. [CrossRef]
49. Bansal, K.; Kumar, S.; Singh, A.; Chaudhary, A.; Patil, P.B. Redefining the Taxonomic Boundaries of Genus *Xanthomonas*. *Taxonomy* **2023**, *3*, 452–465. [CrossRef]
50. Aliyu, H.; Lebre, P.; Blom, J.; Cowan, D.; De Maayer, P. Phylogenomic Re-Assessment of the Thermophilic Genus *Geobacillus*. *Syst. Appl. Microbiol.* **2016**, *39*, 527–533. [CrossRef]
51. Sangal, V.; Goodfellow, M.; Blom, J.; Tan, G.Y.A.; Klenk, H.-P.; Sutcliffe, I.C. Revisiting the Taxonomic Status of the Biomedically and Industrially Important Genus Amycolatopsis, Using a Phylogenomic Approach. *Front. Microbiol.* **2018**, *9*, 2281. [CrossRef]
52. Altschul, S.F.; Gish, W.; Miller, W.; Myers, E.W.; Lipman, D.J. Basic Local Alignment Search Tool. *J. Mol. Biol.* **1990**, *215*, 403–410. [CrossRef]
53. Lindsey, R.L.; Gladney, L.M.; Huang, A.D.; Griswold, T.; Katz, L.S.; Dinsmore, B.A.; Im, M.S.; Kucerova, Z.; Smith, P.A.; Lane, C.; et al. Rapid Identification of Enteric Bacteria from Whole Genome Sequences Using Average Nucleotide Identity Metrics. *Front. Microbiol.* **2023**, *14*, 1225207. [CrossRef] [PubMed]
54. Jain, C.; Rodriguez-R, L.M.; Phillippy, A.M.; Konstantinidis, K.T.; Aluru, S. High Throughput ANI Analysis of 90K Prokaryotic Genomes Reveals Clear Species Boundaries. *Nat. Commun.* **2018**, *9*, 5114. [CrossRef]
55. Ondov, B.D.; Treangen, T.J.; Melsted, P.; Mallonee, A.B.; Bergman, N.H.; Koren, S.; Phillippy, A.M. Mash: Fast Genome and Metagenome Distance Estimation Using MinHash. *Genome. Biol.* **2016**, *17*, 132. [CrossRef]
56. Noble, P.A.; Citek, R.W.; Ogunseitan, O.A. Tetranucleotide Frequencies in Microbial Genomes. *Electrophoresis* **1998**, *19*, 528–535. [CrossRef]
57. Richter, M.; Rosselló-Móra, R.; Oliver Glöckner, F.; Peplies, J. JSpeciesWS: A Web Server for Prokaryotic Species Circumscription Based on Pairwise Genome Comparison. *Bioinformatics* **2016**, *32*, 929–931. [CrossRef] [PubMed]
58. Burall, L.S.; Grim, C.J.; Mammel, M.K.; Datta, A.R. Whole Genome Sequence Analysis Using JSpecies Tool Establishes Clonal Relationships between *Listeria monocytogenes* Strains from Epidemiologically Unrelated Listeriosis Outbreaks. *PLoS ONE* **2016**, *11*, e0150797. [CrossRef]
59. Abe, T.; Kanaya, S.; Kinouchi, M.; Ichiba, Y.; Kozuki, T.; Ikemura, T. Informatics for Unveiling Hidden Genome Signatures. *Genome. Res.* **2003**, *13*, 693–702. [CrossRef] [PubMed]
60. Bohlin, J.; Skjerve, E.; Ussery, D.W. Reliability and Applications of Statistical Methods Based on Oligonucleotide Frequencies in Bacterial and Archaeal Genomes. *BMC Genom.* **2008**, *9*, 104. [CrossRef] [PubMed]
61. Pride, D.T.; Meinersmann, R.J.; Wassenaar, T.M.; Blaser, M.J. Evolutionary Implications of Microbial Genome Tetranucleotide Frequency Biases. *Genome Res.* **2003**, *13*, 145–158. [CrossRef] [PubMed]
62. Richter, M.; Rosselló-Móra, R. Shifting the Genomic Gold Standard for the Prokaryotic Species Definition. *Proc. Natl. Acad. Sci. USA* **2009**, *106*, 19126–19131. [CrossRef]
63. Nakano, Y.; Domon, Y.; Yamagishi, K. Phylogenetic Trees of Closely Related Bacterial Species and Subspecies Based on Frequencies of Short Nucleotide Sequences. *PLoS ONE* **2023**, *18*, e0268847. [CrossRef]
64. Takahashi, M.; Kryukov, K.; Saitou, N. Estimation of Bacterial Species Phylogeny through Oligonucleotide Frequency Distances. *Genomics* **2009**, *93*, 525–533. [CrossRef]
65. Yamao, F.; Muto, A.; Kawauchi, Y.; Iwami, M.; Iwagami, S.; Azumi, Y.; Osawa, S. UGA Is Read as Tryptophan in *Mycoplasma capricolum*. *Proc. Natl. Acad. Sci. USA* **1985**, *82*, 2306–2309. [CrossRef]
66. Renaudin, J.; Pascarel, M.-C.; Saillard, C.; Chevalier, C.; Bove, J.-M. Chez Les Spiroplasmes Le Codon UGA N'Est Pas Non Sens et Semble Coder Pour Le Tryptophane. *C. R. Acad. Sci.* **1986**, *303*, 539–540.
67. Inamine, J.M.; Ho, K.C.; Loechel, S.; Hu, P.C. Evidence That UGA Is Read as a Tryptophan Codon Rather than as a Stop Codon by *Mycoplasma pneumoniae*, *Mycoplasma genitalium*, and *Mycoplasma gallisepticum*. *J. Bacteriol.* **1990**, *172*, 504–506. [CrossRef]
68. Tanaka, R.; Muto, A.; Osawa, S. Nucleotide Sequence of Tryptophan tRNA Gene in *Acholeplasma laidlawii*. *Nucleic Acids Res.* **1989**, *17*, 5842. [CrossRef]
69. Spencer, P.S.; Siller, E.; Anderson, J.F.; Barral, J.M. Silent Substitutions Predictably Alter Translation Elongation Rates and Protein Folding Efficiencies. *J. Mol. Biol.* **2012**, *422*, 328–335. [CrossRef]
70. Yu, C.-H.; Dang, Y.; Zhou, Z.; Wu, C.; Zhao, F.; Sachs, M.S.; Liu, Y. Codon Usage Influences the Local Rate of Translation Elongation to Regulate Co-Translational Protein Folding. *Mol. Cell* **2015**, *59*, 744–754. [CrossRef]

71. Presnyak, V.; Alhusaini, N.; Chen, Y.-H.; Martin, S.; Morris, N.; Kline, N.; Olson, S.; Weinberg, D.; Baker, K.E.; Graveley, B.R.; et al. Codon Optimality Is a Major Determinant of mRNA Stability. *Cell* **2015**, *160*, 1111–1124. [CrossRef]
72. Sharp, P.M.; Li, W.-H. An Evolutionary Perspective on Synonymous Codon Usage in Unicellular Organisms. *J. Mol. Evol.* **1986**, *24*, 28–38. [CrossRef] [PubMed]
73. Miller, J.B.; Hippen, A.A.; Belyeu, J.R.; Whiting, M.F.; Ridge, P.G. Missing Something? Codon Aversion as a New Character System in Phylogenetics. *Cladistics* **2017**, *33*, 545–556. [CrossRef] [PubMed]
74. Vesth, T.; Lagesen, K.; Acar, Ö.; Ussery, D. CMG-Biotools, a Free Workbench for Basic Comparative Microbial Genomics. *PLoS ONE* **2013**, *8*, e60120. [CrossRef] [PubMed]
75. Shen, W.; Le, S.; Li, Y.; Hu, F. SeqKit: A Cross-Platform and Ultrafast Toolkit for FASTA/Q File Manipulation. *PLoS ONE* **2016**, *11*, e0163962. [CrossRef]
76. R Core Team. *R: A Language and Environment for Statistical Computing*, version R v4.4.2; R Foundation for Statistical Computing: Vienna, Austria, 2024.
77. Taskesen, E. *Interactive and Standalone Heatmaps (d3heatmap)*, version 0.1.7; Zenodo: Geneva, Switzerland, 2019. [CrossRef]
78. Garnier, S.; Ross, N.; Rudis, B.; Sciaini, M.; Camargo, A.; Scherer, C. *viridis(Lite)—Colorblind-Friendly Color Maps for R*, version 0.6.5; Zenodo: Geneva, Switzerland, 2024. [CrossRef]
79. Hyatt, D.; Chen, G.-L.; LoCascio, P.F.; Land, M.L.; Larimer, F.W.; Hauser, L.J. Prodigal: Prokaryotic Gene Recognition and Translation Initiation Site Identification. *BMC Bioinform.* **2010**, *11*, 119. [CrossRef]
80. Lagesen, K.; Hallin, P.; Rødland, E.A.; Stærfeldt, H.-H.; Rognes, T.; Ussery, D.W. RNAmmer: Consistent and Rapid Annotation of Ribosomal RNA Genes. *Nucleic Acids Res.* **2007**, *35*, 3100–3108. [CrossRef]
81. Zhao, Y.; Wei, W.; Lee, I.-M.; Shao, J.; Suo, X.; Davis, R.E. Construction of an Interactive Online Phytoplasma Classification Tool, iPhyClassifier, and Its Application in Analysis of the Peach X-Disease Phytoplasma Group (16SrIII). *Int. J. Syst. Evol. Microbiol.* **2009**, *59*, 2582–2593. [CrossRef]
82. Zhao, Y.; Wei, W.; Lee, I.-M.; Shao, J.; Suo, X.; Davis, R.E. The iPhyClassifier, an Interactive Online Tool for Phytoplasma Classification and Taxonomic Assignment. In *Phytoplasma: Methods and Protocols*; Dickinson, M., Hodgetts, J., Eds.; Humana Press: Totowa, NJ, USA, 2013; pp. 329–338.
83. Boratyn, G.M.; Camacho, C.; Cooper, P.S.; Coulouris, G.; Fong, A.; Ma, N.; Madden, T.L.; Matten, W.T.; McGinnis, S.D.; Merezhuk, Y.; et al. BLAST: A More Efficient Report with Usability Improvements. *Nucleic Acids Res.* **2013**, *41*, W29–W33. [CrossRef]
84. Simão, F.A.; Waterhouse, R.M.; Ioannidis, P.; Kriventseva, E.V.; Zdobnov, E.M. BUSCO: Assessing Genome Assembly and Annotation Completeness with Single-Copy Orthologs. *Bioinformatics* **2015**, *31*, 3210–3212. [CrossRef] [PubMed]
85. Shimoyama, Y. COGclassifier: A Tool for Classifying Prokaryote Protein Sequences into COG Funcional Category. 2022. Available online: https://github.com/moshi4/COGclassifier (accessed on 7 December 2024).
86. Edgar, R.C. MUSCLE: A Multiple Sequence Alignment Method with Reduced Time and Space Complexity. *BMC Bioinform.* **2004**, *5*, 113. [CrossRef] [PubMed]
87. Minh, B.Q.; Schmidt, H.A.; Chernomor, O.; Schrempf, D.; Woodhams, M.D.; von Haeseler, A.; Lanfear, R. IQ-TREE 2: New Models and Efficient Methods for Phylogenetic Inference in the Genomic Era. *Mol. Biol. Evol.* **2020**, *37*, 1530–1534. [CrossRef] [PubMed]
88. Tamura, K.; Stecher, G.; Kumar, S. MEGA11: Molecular Evolutionary Genetics Analysis Version 11. *Mol. Biol. Evol.* **2021**, *38*, 3022–3027. [CrossRef]
89. Chaumeil, P.-A.; Mussig, A.J.; Hugenholtz, P.; Parks, D.H. GTDB-Tk: A Toolkit to Classify Genomes with the Genome Taxonomy Database. *Bioinformatics* **2020**, *36*, 1925–1927. [CrossRef]
90. Letunic, I.; Bork, P. Interactive Tree Of Life (iTOL): An Online Tool for Phylogenetic Tree Display and Annotation. *Bioinformatics* **2007**, *23*, 127–128. [CrossRef]
91. Volokhov, D.V.; Neverov, A.A.; George, J.; Kong, H.; Liu, S.X.; Anderson, C.; Davidson, M.K.; Chizhikov, V. Genetic Analysis of Housekeeping Genes of Members of the Genus *Acholeplasma*: Phylogeny and Complementary Molecular Markers to the 16S rRNA Gene. *Mol. Phylogenet. Evol.* **2007**, *44*, 699–710. [CrossRef]
92. Wang, R.; Bai, B.; Li, D.; Wang, J.; Huang, W.; Wu, Y.; Zhao, L. Phytoplasma: A Plant Pathogen That Cannot Be Ignored in Agricultural Production-Research Progress and Outlook. *Mol. Plant Pathol.* **2024**, *25*, e13437. [CrossRef]
93. Huang, C.-T.; Cho, S.-T.; Lin, Y.-C.; Tan, C.-M.; Chiu, Y.-C.; Yang, J.-Y.; Kuo, C.-H. Comparative Genome Analysis of '*Candidatus* Phytoplasma luffae' Reveals the Influential Roles of Potential Mobile Units in Phytoplasma Evolution. *Front. Microbiol.* **2022**, *13*, 773608. [CrossRef]
94. Toth, R.; Huettel, B.; Eini, O.; Varrelmann, M.; Kube, M. The Complete Genome Sequence of the Stolbur Pathogen '*Candidatus* Phytoplasma solani' from *Pentastiridius leporinus*. *Microbiol. Resour. Announc.* **2024**, *14*, e00640-24. [CrossRef]
95. Rodrigues Jardim, B.; Tran-Nguyen, L.T.T.; Gambley, C.; Al-Sadi, A.M.; Al-Subhi, A.M.; Foissac, X.; Salar, P.; Cai, H.; Yang, J.-Y.; Davis, R.; et al. The Observation of Taxonomic Boundaries for the 16SrII and 16SrXXV Phytoplasmas Using Genome-Based Delimitation. *Int. J. Syst. Evol. Microbiol.* **2023**, *73*, 005977. [CrossRef]

96. Safarova, D.; Navratil, M.; Válová, P.; Zemanek, T. '*Candidatus* Phytoplasma cirsii', a Novel Taxon from Creeping Thistle (*Cirsium arvense* (L.) Scop.). *Int. J. Syst. Evol. Microbiol.* **2016**, *66*, 1745–1753. [CrossRef]
97. Watcharachaiyakup, J.; Burns, P.; Chaphakdee, P.; Boonsonti, W.; Saengmanee, P.; Kositratana, W. Multilocus Genotyping of Sugarcane White Leaf Phytoplasma in Thailand. *Trop. Plant Pathol.* **2024**, *49*, 346–356. [CrossRef]
98. Kriventseva, E.V.; Kuznetsov, D.; Tegenfeldt, F.; Manni, M.; Dias, R.; Simão, F.A.; Zdobnov, E.M. OrthoDB V10: Sampling the Diversity of Animal, Plant, Fungal, Protist, Bacterial and Viral Genomes for Evolutionary and Functional Annotations of Orthologs. *Nucleic Acids Res.* **2019**, *47*, D807–D811. [CrossRef] [PubMed]
99. Valverde, R.; Edwards, L.; Regan, L. Structure and Function of KH Domains. *FEBS J.* **2008**, *275*, 2712–2726. [CrossRef]
100. Eriani, G.; Dirheimer, G.; Gangloff, J. Cysteinyl-tRNA Synthetase: Determination of the Last E.Coli Aminoacyl-tRNA Synthetase Primary Structure. *Nucleic Acids Res.* **1991**, *19*, 265–269. [CrossRef] [PubMed]
101. Gualerzi, C.O.; Pon, C.L. Initiation of mRNA Translation in Prokaryotes. *Biochemistry* **1990**, *29*, 5881–5889. [CrossRef] [PubMed]
102. Lee, I.; Suzuki, C.K. Functional Mechanics of the ATP-Dependent Lon Protease- Lessons from Endogenous Protein and Synthetic Peptide Substrates. *Biochim. Biophys. Acta* **2008**, *1784*, 727–735. [CrossRef]
103. Luirink, J.; Sinning, I. SRP-Mediated Protein Targeting: Structure and Function Revisited. *Biochim. Biophys. Acta* **2004**, *1694*, 17–35. [CrossRef] [PubMed]
104. Marians, K.J.; Hiasa, H.; Kim, D.R.; McHenry, C.S. Role of the Core DNA Polymerase III Subunits at the Replication Fork: α is the only subunit required for processive replication. *J. Biol. Chem.* **1998**, *273*, 2452–2457. [CrossRef] [PubMed]
105. Parks, D.H.; Chuvochina, M.; Waite, D.W.; Rinke, C.; Skarshewski, A.; Chaumeil, P.-A.; Hugenholtz, P. A Standardized Bacterial Taxonomy Based on Genome Phylogeny Substantially Revises the Tree of Life. *Nat. Biotechnol.* **2018**, *36*, 996–1004. [CrossRef] [PubMed]
106. Duduk, B.; Ćurčić, Ž.; Stepanović, J.; Böhm, J.W.; Kosovac, A.; Rekanović, E.; Kube, M. Prevalence of a '*Candidatus* Phytoplasma solani'-Related Strain Designated as New 16SrXII-P Subgroup over '*Candidatus* Arsenophonus phytopathogenicus' in Sugar Beet in Eastern Germany. *Plant Dis.* **2023**, *107*, 3792–3800. [CrossRef]
107. Toth, R.; Huettel, B.; Varrelmann, M.; Kube, M. The 16SrXII-P Phytoplasma GOE Is Separated from Other Stolbur Phytoplasmas by Key Genomic Features. *Pathogens* **2025**, *14*, 180. [CrossRef]
108. Pei, A.Y.; Oberdorf, W.E.; Nossa, C.W.; Agarwal, A.; Chokshi, P.; Gerz, E.A.; Jin, Z.; Lee, P.; Yang, L.; Poles, M.; et al. Diversity of 16S rRNA Genes within Individual Prokaryotic Genomes. *Appl. Environ. Microbiol.* **2010**, *76*, 3886–3897. [CrossRef]
109. Kitahara, K.; Miyazaki, K. Revisiting Bacterial Phylogeny. *Mob. Genet. Elements* **2013**, *3*, e24210. [CrossRef]
110. Kiepas, A.B.; Hoskisson, P.A.; Pritchard, L. 16S rRNA Phylogeny and Clustering Is Not a Reliable Proxy for Genome-Based Taxonomy in Streptomyces. *Microb. Genom.* **2024**, *10*, 001287. [CrossRef]
111. Spergser, J.; DeSoye, P.; Ruppitsch, W.; Cabal Rosel, A.; Dinhopl, N.; Szostak, M.P.; Loncaric, I.; Chopra-Dewasthaly, R.; Busse, H.-J. *Mycoplasma tauri* sp. nov. Isolated from the Bovine Genital Tract. *Syst. Appl. Microbiol.* **2022**, *45*, 126292. [CrossRef]
112. Volokhov, D.V.; Furtak, V.A.; Blom, J.; Zagorodnyaya, T.A.; Gao, Y.; Gulland, F.M. *Mycoplasma miroungirhinis* sp. nov. and *Mycoplasma miroungigenitalium* sp. nov., Isolated from Northern Elephant Seals (*Mirounga angustirostris*), *Mycoplasma phocoenae* sp. nov., Isolated from Harbour Porpoise (*Phocoena phocoena*), and *Mycoplasma phocoeninasale* sp. nov., Isolated from Harbour Porpoise and California Sea Lions (*Zalophus californianus*). *Int. J. Syst. Evol. Microbiol.* **2022**, *72*, 005224. [CrossRef]
113. Fischer, L.; Möller Palau-Ribes, F.; Enderlein, D.; Fischer, D.; Herbst, W.; Baudler, L.; Hafez, H.M.; Lierz, M. Corrigendum to "Description, Occurrence and Significance of *Mycoplasma seminis* sp. nov. Isolated from Semen of a Gyrfalcon (*Falco rusticolus*)". *Vet. Microbiol.* **2020**, *249*, 108800. [CrossRef]
114. Spergser, J.; Botes, A.; Nel, T.; Ruppitsch, W.; Lepuschitz, S.; Langer, S.; Ries, S.; Dinhopl, N.; Szostak, M.; Loncaric, I.; et al. *Mycoplasma nasistruthionis* sp. nov. and *Mycoplasma struthionis* sp. nov. Isolated from Ostriches with Respiratory Disease. *Syst. Appl. Microbiol.* **2020**, *43*, 126047. [CrossRef] [PubMed]
115. Volokhov, D.V.; Grózner, D.; Gyuranecz, M.; Ferguson-Noel, N.; Gao, Y.; Bradbury, J.M.; Whittaker, P.; Chizhikov, V.E.; Szathmary, S.; Stipkovits, L. *Mycoplasma anserisalpingitidis* sp. nov., Isolated from European Domestic Geese (*Anser anser domesticus*) with Reproductive Pathology. *Int. J. Syst. Evol. Microbiol.* **2020**, *70*, 2369–2381. [CrossRef]
116. Oren, A.; Garrity, G.M. List of New Names and New Combinations Previously Effectively, but Not Validly, Published. *Int. J. Syst. Evol. Microbiol.* **2018**, *68*, 3379–3393. [CrossRef]
117. Alvarez-Ponce, D.; Weitzman, C.; Tillett, R.; Sandmeier, F.; Tracy, R. High Quality Draft Genome Sequences of *Mycoplasma agassizii* Strains PS6T and 723 Isolated from *Gopherus tortoises* with Upper Respiratory Tract Disease. *Stand. Genomic Sci.* **2018**, *13*, 12. [CrossRef]
118. Ramírez, A.S.; Poveda, J.B.; Dijkman, R.; Poveda, C.; Suárez-Pérez, A.; Rosales, R.S.; Feberwee, A.; Szostak, M.P.; Ressel, L.; Viver, T.; et al. *Mycoplasma bradburyae* sp. nov. Isolated from the Trachea of Sea Birds. *Syst. Appl. Microbiol.* **2023**, *46*, 126472. [CrossRef] [PubMed]
119. Yavari, C.A.; Ramírez, A.S.; Nicholas, R.A.J.; Radford, A.D.; Darby, A.C.; Bradbury, J.M. *Mycoplasma tullyi* sp. nov., Isolated from Penguins of the Genus *Spheniscus*. *Int. J. Syst. Evol. Microbiol.* **2017**, *67*, 3692–3698. [CrossRef]

120. Johansson, K.E.; Tully, J.G.; Bölske, G.; Pettersson, B. *Mycoplasma cavipharyngis* and *Mycoplasma fastidiosum*, the Closest Relatives to *Eperythrozoon* spp. and *Haemobartonella* spp. *FEMS Microbiol. Lett.* **1999**, *174*, 321–326. [CrossRef] [PubMed]
121. Gasparich, G.; Kuo, C.-H. Genome Analysis-Based Union of the Genus *Mesoplasma* with the Genus *Entomoplasma*. *Int. J. Syst. Evol. Microbiol.* **2019**, *69*, 2735–2738. [CrossRef]
122. Chang, T.-H.; Lo, W.-S.; Ku, C.; Chen, L.-L.; Kuo, C.-H. Molecular Evolution of the Substrate Utilization Strategies and Putative Virulence Factors in Mosquito-Associated *Spiroplasma* Species. *Genome Biol. Evol.* **2014**, *6*, 500–509. [CrossRef]
123. Lo, W.-S.; Gasparich, G.; Kuo, C.-H. Found and Lost: The Fates of Horizontally Acquired Genes in Arthropod-Symbiotic *Spiroplasma*. *Genome Biol. Evol.* **2015**, *7*, 2458–2472. [CrossRef]
124. Volokhov, D.V.; Furtak, V.A.; Zagorodnyaya, T.A.; Gao, Y.; Davidson, M.K. *Paracholeplasma manati* sp. nov. Isolated from Florida Manatees (*Trichechus manatus latirostris*). *Int. J. Syst. Evol. Microbiol.* **2023**, *73*, 005973. [CrossRef] [PubMed]
125. Kirdat, K.; Tiwarekar, B.; Sathe, S.; Yadav, A. From Sequences to Species: Charting the Phytoplasma Classification and Taxonomy in the Era of Taxogenomics. *Front. Microbiol.* **2023**, *14*, 1123783. [CrossRef]
126. Murray, R.G.E.; Schleifer, K.H. Taxonomic Notes: A Proposal for Recording the Properties of Putative Taxa of Procaryotes. *Int. J. Syst. Evol. Microbiol.* **1994**, *44*, 174–176. [CrossRef]
127. The IRPCM Phytoplasma/Spiroplasma Working Team—Phytoplasma Taxonomy Group. '*Candidatus* Phytoplasma', a Taxon for the Wall-Less, Non-Helical Prokaryotes That Colonize Plant Phloem and Insects. *Int. J. Syst. Evol. Microbiol.* **2004**, *54*, 1243–1255. [CrossRef]
128. ICSB Subcommittee on the Taxonomy of *Mycoplasmatales*. Proposal for Minimal Standards for Descriptions of New Species of the Order *Mycoplasmatales*. *Int. J. Syst. Evol. Microbiol.* **1972**, *22*, 184–188. [CrossRef]
129. ICSB Subcommittee on the Taxonomy of *Mollicutes*. Proposal of Minimal Standards for Descriptions of New Species of the Class *Mollicutes*: International Committee on Systematic Bacteriology Subcommittee on the Taxonomy of *Mollicutes*. *Int. J. Syst. Evol. Microbiol.* **1979**, *29*, 172–180. [CrossRef]
130. ICSB Subcommittee on the Taxonomy of *Mollicutes*. Revised Minimum Standards for Description of New Species of the Class *Mollicutes* (Division Tenericutes). *Int. J. Syst. Evol. Microbiol.* **1995**, *45*, 605–612. [CrossRef]
131. Weisburg, W.G.; Tully, J.G.; Rose, D.L.; Petzel, J.P.; Oyaizu, H.; Yang, D.; Mandelco, L.; Sechrest, J.; Lawrence, T.G.; Van Etten, J. A Phylogenetic Analysis of the Mycoplasmas: Basis for Their Classification. *J. Bacteriol.* **1989**, *171*, 6455–6467. [CrossRef]
132. Stackebrandt, E.; Frederiksen, W.; Garrity, G.M.; Grimont, P.A.D.; Kämpfer, P.; Maiden, M.C.J.; Nesme, X.; Rosselló-Mora, R.; Swings, J.; Trüper, H.G.; et al. Report of the Ad Hoc Committee for the Re-Evaluation of the Species Definition in Bacteriology. *Int. J. Syst. Evol. Microbiol.* **2002**, *52*, 1043–1047. [CrossRef]
133. Clarridge, J.E. Impact of 16S rRNA Gene Sequence Analysis for Identification of Bacteria on Clinical Microbiology and Infectious Diseases. *Clin. Microbiol. Rev.* **2004**, *17*, 840–862. [CrossRef] [PubMed]
134. Grosjean, H.; Breton, M.; Sirand-Pugnet, P.; Tardy, F.; Thiaucourt, F.; Citti, C.; Barré, A.; Yoshizawa, S.; Fourmy, D.; de Crécy-Lagard, V.; et al. Predicting the Minimal Translation Apparatus: Lessons from the Reductive Evolution of *Mollicutes*. *PLoS Genet.* **2014**, *10*, e1004363. [CrossRef]
135. Sirand-Pugnet, P.; Lartigue, C.; Marenda, M.; Jacob, D.; Barré, A.; Barbe, V.; Schenowitz, C.; Mangenot, S.; Couloux, A.; Segurens, B.; et al. Being Pathogenic, Plastic, and Sexual While Living with a Nearly Minimal Bacterial Genome. *PLoS Genet.* **2007**, *3*, e75. [CrossRef] [PubMed]
136. Pereyre, S.; Sirand-Pugnet, P.; Beven, L.; Charron, A.; Renaudin, H.; Barré, A.; Avenaud, P.; Jacob, D.; Couloux, A.; Barbe, V.; et al. Life on Arginine for *Mycoplasma hominis*: Clues from Its Minimal Genome and Comparison with Other Human Urogenital Mycoplasmas. *PLoS Genet.* **2009**, *5*, e1000677. [CrossRef] [PubMed]
137. Rocha, E.P.C.; Cornet, E.; Michel, B. Comparative and Evolutionary Analysis of the Bacterial Homologous Recombination Systems. *PLoS Genet.* **2005**, *1*, e15. [CrossRef]
138. Sirand-Pugnet, P.; Citti, C.; Barré, A.; Blanchard, A. Evolution of *Mollicutes*: Down a Bumpy Road with Twists and Turns. *Res. Microbiol.* **2007**, *158*, 754–766. [CrossRef]
139. Citti, C.; Dordet-Frisoni, E.; Nouvel, L.X.; Kuo, C.H.; Baranowski, E. Horizontal Gene Transfers in Mycoplasmas (*Mollicutes*). *Curr. Issues Mol. Biol.* **2018**, *29*, 3–22. [CrossRef]
140. Oren, A.; Garrity, G.M. List of New Names and New Combinations Previously Effectively, but Not Validly, Published. *Int. J. Syst. Evol. Microbiol.* **2019**, *69*, 597–599. [CrossRef]
141. Balish, M.; Bertaccini, A.; Blanchard, A.; Brown, D.; Browning, G.; Chalker, V.; Frey, J.; Gasparich, G.; Hoelzle, L.; Knight, T.; et al. Recommended Rejection of the Names *Malacoplasma* gen. nov., *Mesomycoplasma* gen. nov., *Metamycoplasma* gen. nov., *Metamycoplasmataceae* fam. nov., *Mycoplasmoidaceae* fam. nov., *Mycoplasmoidales* ord. nov., *Mycoplasmoides* gen. nov., *Mycoplasmopsis* gen. nov. [Gupta, Sawnani, Adeolu, Alnajar and Oren 2018] and All Proposed Species Comb. Nov. Placed Therein. *Int. J. Syst. Evol. Microbiol.* **2019**, *69*, 3650–3653. [CrossRef]

142. Freese, H.M.; Meier-Kolthoff, J.P.; Sardà Carbasse, J.; Afolayan, A.O.; Göker, M. TYGS and LPSN in 2025: A Global Core Biodata Resource for Genome-Based Classification and Nomenclature of Prokaryotes within DSMZ Digital Diversity. *Nucleic Acids Res.* **2026**, *54*, D884–D891. [CrossRef]
143. Iriarte, A.; Baraibar, J.D.; Romero, H.; Musto, H. Selected Codon Usage Bias in Members of the Class *Mollicutes*. *Gene* **2011**, *473*, 110–118. [CrossRef]
144. Lim, P.O.; Sears, B.B. Evolutionary Relationships of a Plant-Pathogenic Mycoplasmalike Organism and *Acholeplasma laidlawii* Deduced from Two Ribosomal Protein Gene Sequences. *J. Bacteriol.* **1992**, *174*, 2606–2611. [CrossRef] [PubMed]
145. Karlin, S.; Bucher, P. Correlation Analysis of Amino Acid Usage in Protein Classes. *Proc. Natl. Acad. Sci. USA* **1992**, *89*, 12165–12169. [CrossRef] [PubMed]
146. Iriarte, A.; Baraibar, J.D.; Diana, L.; Castro-Sowinski, S.; Romero, H.; Musto, H. Trends in Amino Acid Usage across the Class *Mollicutes*. *J. Biomol. Struct. Dyn.* **2014**, *32*, 65–74. [CrossRef] [PubMed]
147. Liò, P.; Goldman, N. Models of Molecular Evolution and Phylogeny. *Genome Res.* **1998**, *8*, 1233–1244. [CrossRef]
148. Miller, J.B.; McKinnon, L.M.; Whiting, M.F.; Ridge, P.G. Codon Use and Aversion Is Largely Phylogenetically Conserved across the Tree of Life. *Mol. Phylogenet. Evol.* **2020**, *144*, 106697. [CrossRef]
149. Novoa, E.M.; Jungreis, I.; Jaillon, O.; Kellis, M. Elucidation of Codon Usage Signatures across the Domains of Life. *Mol. Biol. Evol.* **2019**, *36*, 2328–2339. [CrossRef]
150. Větrovský, T.; Baldrian, P. The Variability of the 16S rRNA Gene in Bacterial Genomes and Its Consequences for Bacterial Community Analyses. *PLoS ONE* **2013**, *8*, e57923. [CrossRef]
151. Tazzyman, S.J.; Bonhoeffer, S. Why There Are No Essential Genes on Plasmids. *Mol. Biol. Evol.* **2015**, *32*, 3079–3088. [CrossRef]
152. Emms, D.M.; Kelly, S. OrthoFinder: Phylogenetic Orthology Inference for Comparative Genomics. *Genome Biol.* **2019**, *20*, 238. [CrossRef]
153. Hug, L.A.; Baker, B.J.; Anantharaman, K.; Brown, C.T.; Probst, A.J.; Castelle, C.J.; Butterfield, C.N.; Hernsdorf, A.W.; Amano, Y.; Ise, K.; et al. A New View of the Tree of Life. *Nat. Microbiol.* **2016**, *1*, 16048. [CrossRef]
154. Barco, R.A.; Garrity, G.M.; Scott, J.J.; Amend, J.P.; Nealson, K.H.; Emerson, D. A Genus Definition for Bacteria and Archaea Based on a Standard Genome Relatedness Index. *mBio* **2020**, *11*, e02475-19. [CrossRef] [PubMed]
155. Gasparich, G.E.; Whitcomb, R.F.; Dodge, D.; French, F.E.; Glass, J.; Williamson, D.L. The Genus *Spiroplasma* and Its Non-Helical Descendants: Phylogenetic Classification, Correlation with Phenotype and Roots of the *Mycoplasma mycoides* Clade. *Int. J. Syst. Evol. Microbiol.* **2004**, *54*, 893–918. [CrossRef] [PubMed]

Disclaimer/Publisher's Note: The statements, opinions and data contained in all publications are solely those of the individual author(s) and contributor(s) and not of MDPI and/or the editor(s). MDPI and/or the editor(s) disclaim responsibility for any injury to people or property resulting from any ideas, methods, instructions or products referred to in the content.